# Committed carbon emissions, deforestation, and community land conversion from oil palm plantation expansion in West Kalimantan, Indonesia

Kimberly M. Carlson[a,b,c,1], Lisa M. Curran[a,b,c,d], Dessy Ratnasari[e], Alice M. Pittman[a,b,c], Britaldo S. Soares-Filho[f], Gregory P. Asner[g], Simon N. Trigg[h], David A. Gaveau[b,e], Deborah Lawrence[i], and Hermann O. Rodrigues[f]

[a]School of Forestry and Environmental Studies, Yale University, New Haven, CT 06511; [b]Woods Institute for the Environment, and [c]Department of Anthropology, Stanford University, Stanford, CA 94305; [d]Santa Fe Institute, Santa Fe, NM 87501; [e]Living Landscapes Indonesia, Pontianak, West Kalimantan, 78121, Indonesia; [f]Centro de Sensoriamento Remoto, Universidade Federal de Minas Gerais, Belo Horizonte, 31270-901, Minas Gerais, Brazil; [g]Department of Global Ecology, Carnegie Institution for Science, Stanford, CA 94305; [h]Natural Resources Department, School of Applied Sciences, Cranfield University, Cranfield, Bedfordshire MK43 0AL, England; and [i]Department of Environmental Sciences, University of Virginia, Charlottesville, VA 22904

Edited by Emilio F. Moran, Indiana University, Bloomington, IN, and approved March 20, 2012 (received for review January 10, 2012)

**Industrial agricultural plantations are a rapidly increasing yet largely unmeasured source of tropical land cover change. Here, we evaluate impacts of oil palm plantation development on land cover, carbon flux, and agrarian community lands in West Kalimantan, Indonesian Borneo. With a spatially explicit land change/carbon bookkeeping model, parameterized using high-resolution satellite time series and informed by socioeconomic surveys, we assess previous and project future plantation expansion under five scenarios. Although fire was the primary proximate cause of 1989–2008 deforestation (93%) and net carbon emissions (69%), by 2007–2008, oil palm directly caused 27% of total and 40% of peatland deforestation. Plantation land sources exhibited distinctive temporal dynamics, comprising 81% forests on mineral soils (1994–2001), shifting to 69% peatlands (2008–2011). Plantation leases reveal vast development potential. In 2008, leases spanned ∼65% of the region, including 62% on peatlands and 59% of community-managed lands, yet <10% of lease area was planted. Projecting business as usual (BAU), by 2020 ∼40% of regional and 35% of community lands are cleared for oil palm, generating 26% of net carbon emissions. Intact forest cover declines to 4%, and the proportion of emissions sourced from peatlands increases 38%. Prohibiting intact and logged forest and peatland conversion to oil palm reduces emissions only 4% below BAU, because of continued uncontrolled fire. Protecting logged forests achieves greater carbon emissions reductions (21%) than protecting intact forests alone (9%) and is critical for mitigating carbon emissions. Extensive allocated leases constrain land management options, requiring trade-offs among oil palm production, carbon emissions mitigation, and maintaining community landholdings.**

greenhouse gas emissions | agribusiness | *Elaeis guineensis* | moratorium | REDD+

Global demand for food, biofuels, and natural resources drives capitalized agricultural development, especially for tropical plantations (1–4). Forest and peatland conversion to plantation agriculture may be a substantial source of greenhouse gas (GHG) emissions from land cover change (5, 6), which generates 10–20% of net global GHG emissions (7). By acquiring extensive arable lands, plantations also affect land availability for smallholder farmers and communities, potentially altering local livelihood options (8, 9). Whereas environmental degradation from tropical agribusiness may overwhelm benefits of high-yield plantations for world food security (6, 10), impacts on carbon (C) flux and livelihoods are highly uncertain because locations and land sources for plantations remain largely undocumented.

Complex processes of land acquisition and plantation development unfold across heterogeneous biophysical and sociopolitical landscapes in both time and space. Land cover histories constrain present land use and potential outcomes from agribusiness expansion (11). Discerning the land cover trajectories that precede agribusiness development requires documenting historical land use by various agents, as well as land jurisdiction (12, 13). Longitudinal, regionally informed land cover assessments at high temporal and spatial resolution are essential to capture the land cover sources and dynamic, often-punctuated changes brought about by plantation expansion (14, 15).

Such refined evaluations are critically needed in tropical countries, especially Indonesia. Since 1990, Indonesia has experienced one of the most rapid plantation expansions worldwide. The Agricultural Ministry's records indicate that from 1990 to 2010, oil palm (*Elaeis guineensis*) area increased 600% to 7.8 Mha (16). Over 90% of this development occurred in Sumatra and Indonesian Borneo (Kalimantan) (17), regions that lost ∼40% of lowland forests from 1990 to 2005 (18). As a result of this extensive deforestation, annual GHG emissions in Indonesia—currently among the top 10 national emitters—are sourced predominantly from land cover/land use change (19). However, the locations, patterns, and land cover sources for oil palm plantation expansion; the extent and distribution of undeveloped oil palm leases pending near-term development; and carbon emissions from oil palm agriculture remain largely undocumented (20–22).

To acquire such datasets for tropical regions requires integrating remote sensing products with interdisciplinary methods and analyses (15). Although optical remote sensing satellites such as Landsat have sufficient temporal (∼20 d) and spatial (≤30 m) resolution to detect small land cover patches and punctuated land cover change, they are hampered by cloud cover and cannot be used to map carbon stocks (23, 24). Technologies such as light detection and ranging (LiDAR) and radar are effective for mapping aboveground live biomass (AGB) [metric tons (t) C·ha$^{-1}$] in tropical forests (e.g., refs. 25 and 26), and even belowground carbon in peatlands (27), yet are not available to capture historical (i.e., pre-2000) conditions. As a result of these limitations, carbon flux estimates from land cover change typically rely on multiplying forest area lost by forest AGB (28). However, such measures contain considerable uncertainties because they treat AGB as a discrete rather than a continuous variable, cannot account for carbon flux from land cover change pre- and postdeforestation, and may group multiple land covers into a few broad classes (29). Until carbon flux from land cover change can be directly assessed, a transition-based framework—where emissions and sequestration are estimated for multiple land cover transitions over time and space—is the most robust method to evaluate carbon emissions from agribusiness-related land change (30).

Author contributions: K.M.C., L.M.C., D.R., and S.N.T. designed research; K.M.C., L.M.C., D.R., D.L., and D.A.G. performed research; K.M.C., B.S.S.-F., G.P.A., and H.O.R. contributed new reagents/analytic tools; K.M.C., L.M.C., and A.M.P. analyzed data; and K.M.C. and L.M.C. wrote the paper.

The authors declare no conflict of interest.

This article is a PNAS Direct Submission.

Freely available online through the PNAS open access option.

[1]To whom correspondence should be addressed. E-mail: kimcarlson@gmail.com.

This article contains supporting information online at www.pnas.org/lookup/suppl/doi:10.1073/pnas.1200452109/-/DCSupplemental.

Quantifying carbon stocks for major tropical land covers, including logged forests and existing agricultural lands, presents several major challenges. Since the 1980s, Kalimantan's intact forests experienced massive degradation from logging in federal timber concessions, with related declines in AGB, and subsequent regrowth (12, 14, 31). However, forest degradation from logging is difficult to detect due to its spatial and temporal heterogeneity, and timber volume removed and biomass accumulation from forest regeneration are variable (15, 32). Moreover, rural agrarian communities in Kalimantan maintain considerable landholdings associated with swidden agriculture (9, 33). These managed agricultural lands, common throughout the humid tropics, are characterized by fallow-cropping cycles of land clearing and regrowth that generate substantial, yet heterogeneous and dynamic, carbon stocks (34, 35). Because Kalimantan contains one-third of Indonesia's peatlands, which harbor the most tropical peat carbon worldwide, belowground carbon is also critical (36, 37). Clearing and draining these peatlands produce considerable carbon emissions from peat oxidation and burning (38, 39).

Although oil palm plantations continue to expand (40), the Government of Indonesia (GOI) has pledged to reduce 26% of their projected business-as-usual 2020 GHG emissions (2.5–3 Gt $CO_2$ equivalent) (41). Diverse international initiatives—including Reducing Emissions from Deforestation and forest Degradation (REDD+), industry roundtables (e.g., Roundtable on Sustainable Palm Oil), and multinational donor agreements—seek to reduce carbon emissions or mitigate impacts of tropical agribusiness. Spatially explicit land change models are useful heuristic tools to evaluate the potential of these proposed policies to achieve their intended outcomes (11, 42). Such models facilitate comparisons among future scenarios that may incorporate economic conditions, natural phenomena, company practices, and smallholder decision making. Ideally, scenario modeling identifies unforeseen relationships and outcomes to provide critical insights for evaluating trade-offs among policies and practices.

Given the importance of Indonesia's land-based carbon emissions, and uncertainties surrounding historical and future oil palm development, we developed a longitudinal study of oil palm plantation development (1989–2020) in Ketapang District, West Kalimantan (Fig. 1). This district comprises the full range of land covers found in Kalimantan, has experienced rapid and extensive land cover change from diverse processes and agents (e.g., wildfires, logging, and plantations), and was among the earliest districts to receive private sector oil palm development (~1994). Using this representative region, we (*i*) evaluate how allocated and planted oil palm, including land cover types converted, vary across both space and time; (*ii*) assess the relative contribution of oil palm expansion to deforestation and carbon flux; and (*iii*) model future scenarios of oil palm expansion and forest conservation policies to examine potential effects on land cover, carbon flux, and agrarian community landholdings.

To assess land cover change, we evaluated transitions among land cover classes (Fig. 2) derived from classified Landsat images acquired from 1989 to 2008, supplemented by a 2011 Landsat image with recent oil palm expansion delineated. Then, we modeled the potential effects of future oil palm expansion and forest conservation policies on land cover, carbon flux, and rural agrarian communities from 2008 to 2020. We contrasted five locally informed scenarios of oil palm development: business as usual (BAU), moratoria (M) on oil palm expansion into peatlands and intact (MInt) and previously logged forests (MSec), and forest protection (FP) for intact (FPInt) and previously logged (FPSec) forested lands exempt from oil palm expansion under the moratorium.

## Results

**Oil Palm Development.** In this Ketapang study region, oil palm plantation land clearing was first observed in the 1994 Landsat image. By 2008, plantation area ($n$ = 16 leases) had expanded to occupy 6% of land outside protected areas (PAs) (Fig. 1*A*). Analysis of regional governmental records indicates that median initial oil palm lease clearing occurred 3 y (range 1–6) after the first record of lease application. Because oil palm development is controlled by lease allocation and influenced by market and political conditions, expansion rates were highly punctuated. From 1994 to 1997, all planted oil palm (0.60% of non-PA land area·$y^{-1}$) occurred in leases awarded from 1990 to 1994 ($n$ = 6), predominantly in former logging concessions (14). From 1997 to 2005, a period characterized by political and financial volatility, we observed reduced expansion in active leases (0.04%·$y^{-1}$), and no new leases began clearing. Elevated 2005–2008 clearing rates (1.33%·$y^{-1}$) were facilitated by clearing in 10 new leases distributed since 2003, coupled with relatively high export commodity prices (6). In 2008, 65% of non-PA lands were allocated to oil palm leases ($n$ = 45 leases). However, 91% of these leased lands ($n$ = 29 leases) had yet to begin land preparation and clearing. From 2008 to 2011, 11 leases initiated clearing, driving high conversion rates (2.60%·$y^{-1}$), and oil palm expanded to occupy 14% of non-PA lands (Fig. 1*B*). Eighty percent of allocated lease area remains unplanted, with 61% on peatlands.

**Land Cover Sources for Oil Palm.** From 1989 to 2008, forests were the primary land cover source (49%) for oil palm plantations. Intact forests composed the majority of this conversion (21%), followed by secondary (21%) and logged (7%) forests. In addition, 37% of oil palm replaced agroforests and agricultural fallows. Only 14% of oil palm was sourced from burned/cleared and bare lands. Across the time series, land and soil types sourced for oil palm expansion were dynamic (Fig. 3). From 1994 to 2001, 81% of

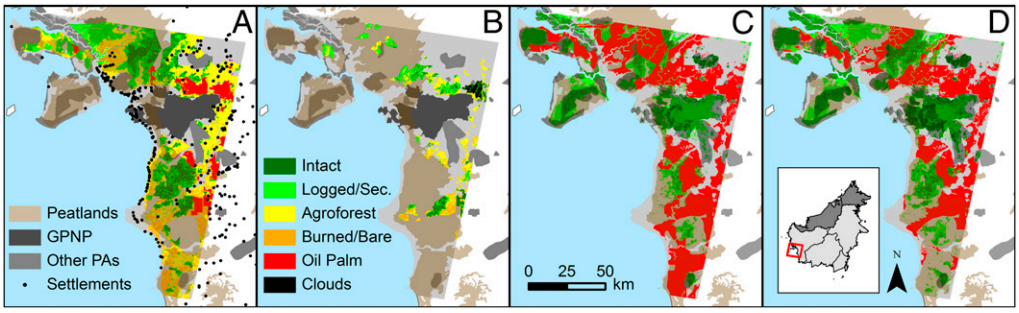


**Fig. 1.** Study region in Ketapang District, West Kalimantan, Indonesia. This coastal region (12,000 $km^2$, Landsat path/row 121/061) contains ~50% peatlands and surrounds Gunung Palung National Park (GPNP, 1,000 $km^2$) and other protected areas (PAs, 1,800 $km^2$). (*A*) 2008 land cover in oil palm leases. Whereas 6% of non-PA lands were cleared for or planted with oil palm, 91% of plantation leases (6,037 $km^2$, $n$ = 45) sited mainly (62%) on peatlands remained undeveloped. (*B*) Land cover sources for oil palm, 1994–2011. Forests (intact, logged, and secondary) were the primary land cover source (49%) for oil palm. By 2011, oil palm spanned 14% of non-PA lands. (*C*) Business-as-usual (BAU) scenario, 2020. Forests cover only 24% of the region, and oil palm occupies 41% of non-PA lands. (*D*) FPSec scenario, 2020. Protection against deforestation and degradation of intact and logged forests in PAs and undeveloped oil palm leases yields 36% greater forest fraction (32% of the region) and 28% lower oil palm area (~30% of non-PA lands) compared with BAU. Future land cover maps (*C* and *D*) were chosen from 60 model runs per scenario.

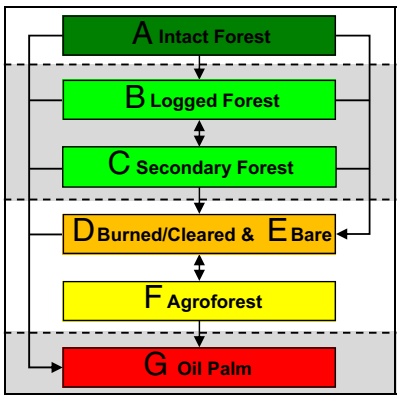


**Fig. 2.** Land cover transitions. Our land cover change simulation, implemented in Dinamica environment for geoprocessing objects (EGO) (51), incorporated dynamic forest degradation (logging), deforestation, and regrowth transitions among seven major land cover classes derived from Landsat satellite data: (*A*) intact forests, closed-canopy natural forests without detectable evidence of disturbance; (*B*) logged forests, natural forests with detectable canopy disturbance; (*C*) secondary forests, recovering logged forests (i.e., not burned, cleared, or relogged after the initial logging event); (*D*) burned and cleared lands, nonforests characterized by recent clearing or burning, including fields burned or cleared for swidden rice production; (*E*) bare lands, including roads, rivers, human settlements, and open mines; (*F*) agroforests and agricultural fallows, swidden agricultural production systems including rice fields, rice fallows, rubber, fruit gardens, and coconut groves, with regrowth on previously burned, cleared, and bare soil areas; (*G*) oil palm, areas cleared for or planted with oil palm. Unidirectional land cover transitions are indicated by dashed lines. For example, although intact forests can be logged, these logged forests cannot return to their previous intact state within the modeled 32-y time series.

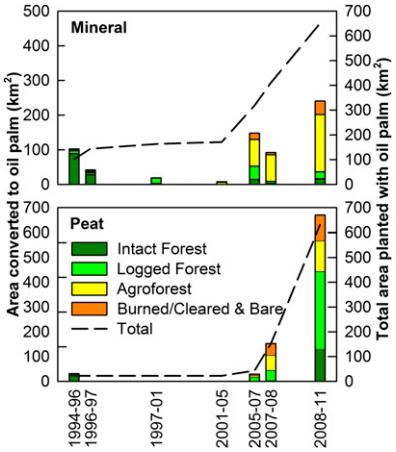


**Fig. 3.** Land cover sources for oil palm plantation establishment and total planted oil palm, from 1994 to 2011. Land cover sources across (*Upper*) mineral and (*Lower*) peat soils were identified by analyzing land cover transitions to oil palm pixels for each time step of the seven-image time series. Oil palm planting began in the Ketapang study region in 1994. Through 2007, oil palm plantations were concentrated on mineral soils. By 2011, 49% of oil palm was planted on peatlands.

plantations were converted from forests on mineral soils. Conversely, from 2001 to 2008, agroforests and nonforests were cleared at the highest rates (72%). Since 2008, forested peatlands composed the largest fraction (44%) of conversion. Through 2007, 73% of oil palm expansion occurred on mineral soils with 27% on peatlands. However, from 2007 to 2008, peatlands composed 54% of conversion, reaching 69% from 2008 to 2011. By 2011, planted oil palm spanned 51% mineral soils and 49% peatlands.

**Forest Cover Loss.** Deforestation—conversion of intact, logged, and secondary forest—averaged 2.9%·y$^{-1}$ from 1989 to 2008 (Table S1). Forest cover outside PAs decreased from 59% to 22%, with especially steep declines in intact forest area (51–6%, Fig. S1). Forest loss peaked at 9.0%·y$^{-1}$ during extensive fires associated with the 1997–1998 El Niño Southern Oscillation (ENSO) (12). Wildfires escaping from oil palm plantations likely contributed to this deforestation; ~8% of total area burned in 1997 occurred <5 km from oil palm. The major proximate causes of forest cover loss were fire related (93%), including transitions to agroforests and agricultural fallows and direct conversion by fire. Whereas only 6% of regional 1994–2008 forest loss could be directly attributed to oil palm expansion, by 2007–2008, 27% of deforestation was ascribed to oil palm, including 40% of all peatland deforestation. Over 50% of forests converted to oil palm had been logged before forest clearing. Although we observed several locations where logging was conducted or contracted by oil palm companies, we did not attribute logging to oil palm development. Our analyses therefore underrepresent the proportion of intact forest loss and associated carbon emissions driven by plantation expansion.

**Land Cover Change Under Land Management Policy Scenarios.** Across oil palm expansion scenarios, by 2020, oil palm covered 29–41% of non-PA lands. Under BAU, 62% of oil palm was planted on peatlands (Fig. 1*C*). However, for all M and FP scenarios, only 46–49% of oil palm was converted from peatlands. Whereas oil palm extent did not differ significantly across M and FP scenarios ($P \geq 0.05$), the FP scenarios conserved significantly higher forest fraction and generated significantly lower burned/cleared and bare fraction than the M scenarios (Fig. 4). The FPSec scenario (Fig. 1*D*) yielded significantly higher forest fraction coupled with significantly lower agroforest and burned/cleared and bare fraction than the FPInt scenario. Land cover class fractions were not significantly different between the MInt and MSec scenarios.

**Carbon Flux.** From 1989 to 2008, total carbon committed to the atmosphere was estimated at 11.4 MtC·y$^{-1}$, with 12.3 MtC·y$^{-1}$ gross emissions, and 0.9 MtC·y$^{-1}$ gross sequestration (Fig. S2). The 1997–1998 ENSO event with associated fires contributed the highest annual net carbon flux (19% of the 20-y total·y$^{-1}$, Fig. 5). Peatlands were the source of 57% of net carbon emissions. The proportion of net carbon flux from peatlands increased from 50% in the 1990s to 68% in the 2000s. The AGB pool yielded 65% of net carbon emissions, whereas peat burning and draining contributed 21% and 14%, respectively. Whereas forest regrowth offset gross carbon emissions in the AGB pool by 2%, agroforest growth offset 9% of these emissions. Land cover transitions mediated by fire composed 69% of net carbon flux, followed by logging (27%). Oil palm emitted only 3% of net carbon from 1994 to 2008 or 4% excluding the 1996–1997 ENSO time step (Fig. S3). Over 75% of gross carbon emissions from oil palm were sourced from clearing AGB in intact, logged, and secondary forests on mineral soils. Peatland deforestation and draining for oil palm contributed relatively few gross emissions (10% and 11%, respectively).

**Carbon Flux Under Land Management Policy Scenarios.** From 2008 to 2020, modeled mean annual carbon flux in the BAU scenario was 11.9 MtC·y$^{-1}$, 14.0 MtC·y$^{-1}$ gross emissions, and 2.1 MtC·y$^{-1}$ gross sequestration (Fig. S2). Both M and FP scenarios showed reductions in net carbon emissions compared with BAU. Excluding oil palm from forests and peatlands under the M scenarios reduced net carbon emissions only 3–4% below BAU. Because so few intact forests remain, protecting secondary and logged forests (FPSec) achieved more than twofold greater carbon reductions (21%) than protecting intact forests alone (FPInt, 9%). Across all scenarios, 86–92% of net carbon emissions originated from peatlands. The peat burning pool contributed 44–52% of carbon flux, with 30–36% attributed to peat draining. The AGB pool contributed only 13–24% of net carbon emissions. Whereas fire-related land cover transitions were the primary cause of carbon flux in all scenarios (67–74%), oil palm was the second leading source of carbon emissions (18–26%, Fig.

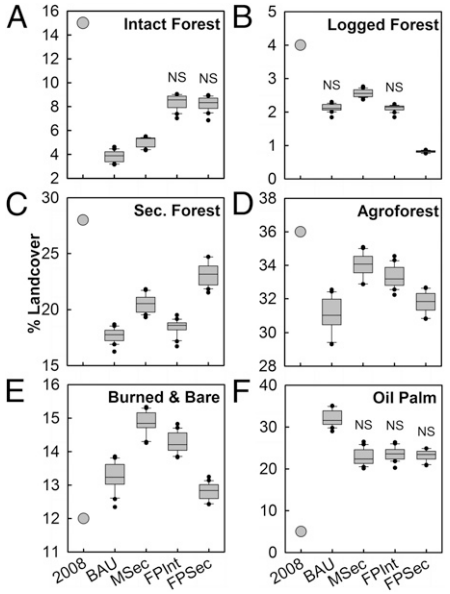


**Fig. 4.** Land cover distribution in 2008 with projections through 2020 for five oil palm expansion scenarios. Land cover is compared for (*A*) intact forests, (*B*) logged forests, (*C*) secondary forests, (*D*) agroforests and agricultural fallows, (*E*) burned/cleared and bare soils, and (*F*) oil palm. Shaded circles denote 2008 land cover. Line demarcates the median of 20 scenario runs; shaded upper and lower bounds indicate 25th/75th percentiles; whiskers represent 10th/90th percentiles. NS indicates nonsignificant ($P \geq 0.05$) differences in land cover fraction between scenarios, measured with paired *t* tests. The MInt scenario (not displayed) did not differ significantly from the MSec scenario for all land cover classes.

S3). Peat draining comprised the greatest source (54–59%) of gross emissions from oil palm, with 26–33% derived from conversion of AGB in intact, logged, and secondary forests on peatlands. Deforestation on mineral soils contributed only 8–12% of gross oil palm emissions. Carbon sequestration from oil palm growth offset only 15% of gross oil palm emissions for the 12-y period in the BAU scenario. Net annual carbon emissions decreased from 2008 to 2020 in all scenarios, driven by declining emissions from peat burning and AGB pools (Fig. 5 *A–D*). In all scenarios except BAU, the AGB pool became a net carbon sink by 2020. Drained peatlands became the primary carbon emissions source in 2020 for the BAU and FPSec scenarios. M and FP scenarios yielded stable levels of emissions from peat draining starting in ~2015, yet draining emissions continued to increase through 2020 under BAU.

**Agrarian Communities.** From our field-generated maps of 247 resident agrarian communities, we estimate that 3,928 $km^2$ of "community-managed lands" (<5 km from settlements, excluding PAs) span this region. Through the early 2000s, community land area converted to oil palm remained low, increasing from 1% in 1996 to 2% in 2005 (Fig. 5*E*). In 2008, community area planted with oil palm expanded to 6%, and 51 surveyed communities (21%) were <5 km from planted oil palm. Moreover, 59% of community-managed lands, representing 191 villages, overlapped oil palm leases. By 2011, community lands occupied by oil palm had more than doubled (13%). By 2020 under BAU, even including a 2-km buffer around settlements preventing oil palm conversion, planted oil palm spanned 35% of community-managed land area. In the best-case FPSec scenario, 28% of community-managed land area was controlled by oil palm plantations in 2020.

## Discussion

**Oil Palm Lease Allocation and Development.** Because oil palm development is characterized by lags between lease allocation—including requests, assessments, and permits—and the onset of landclearing, conversion of allocated oil palm leases alone will generate considerable near-term deforestation and carbon emissions. Although fires were the primary proximate cause (93%) of regional deforestation from 1989 to 2008, since 2007, plantation expansion directly contributed 27% of regional deforestation. Governmental lease records indicate that currently awarded or "committed" oil palm development will be concentrated in peatlands. Whereas ~50% of the Ketapang region spans peatlands, in 2011, 61% of undeveloped lease area was allocated on peatlands. These leases were allocated before the 2011 GOI moratorium on peatland conversion and remain available for oil palm development. BAU scenario results indicate that ~40% of peatlands will be planted with oil palm by 2020, with carbon emissions from peatlands projected to contribute 87% of total emissions under BAU. Existing regulations prohibiting using fire to prepare lands for plantation agriculture, if enforced, may mitigate peat burning emissions. However, oil palm cultivation on peatlands requires draining these soils, resulting in committed carbon emissions from peat oxidation that will continue beyond 2020. Such projections are dependent on the volume of peat losses related to peat drainage depth, characterized by pronounced temporal and spatial heterogeneity and thus considerable uncertainty (38).

**Forest Protection Critical for Carbon Emissions Mitigation.** Critically, outcomes from five policy scenarios indicate that mitigating carbon emissions requires not only prohibiting oil palm expansion into peatlands, but also actively protecting forests in oil palm leases and PAs from all causes of deforestation and degradation. Conservation-based M scenarios reduced 2008–2020 carbon emissions only 3–4% below BAU levels. Merely enforcing a moratorium on converting forests and peatlands to oil palm plantations is predicted to generate negligible carbon emissions

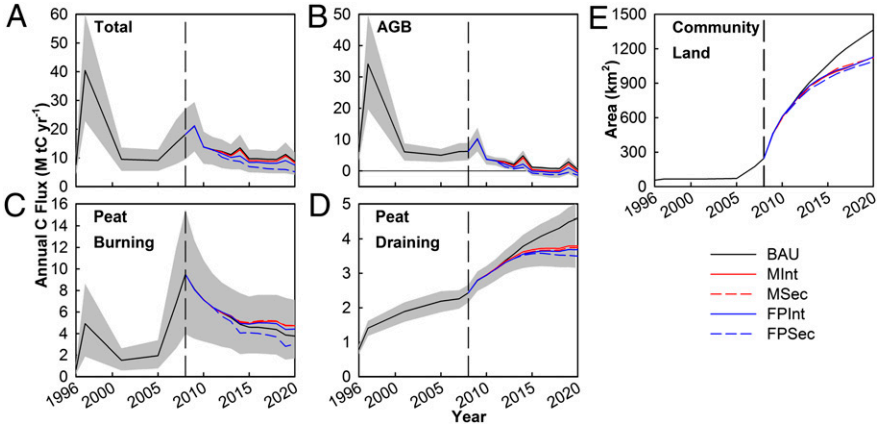


**Fig. 5.** Annual carbon flux and community land area planted with oil palm under five policy scenarios. (*A*) Total carbon emissions peaked in 1997–1998 when ENSO-associated fires burned (*B*) aboveground biomass (AGB) and (*C*) peatlands. (*D*) Carbon emissions from peat draining were a minor contributor to carbon flux pre-2009, but become a major source of emissions by 2020. (*E*) Community land area (<5 km from settlements, excluding PAs) converted to industrial oil palm plantations increased from 6% in 2008 to 28–35% in 2020 across all scenarios. Results from 1989 to 2008 were annualized and then plotted at the final year of each interval. Lines represent means of 20 model runs for each scenario. Gray areas indicate minimum and maximum annual estimated carbon flux derived by applying low and high carbon input values. Positive values indicate carbon emissions; negative values represent carbon sequestration.

reductions because other proximate causes (e.g., wildfires) continue to contribute to forest loss. Moreover, as agroforests are converted to oil palm plantations, smallholder agriculture may be displaced onto forested lands. Compared with BAU, the FP scenarios yielded 9–21% carbon emissions reductions while conserving 22–36% greater forest cover. FP and M scenarios maintained similar plantation area. Most importantly, results from the FPSec scenario reveal that protecting secondary and logged forests, not covered by the GOI moratorium (43), is the strategy that most effectively reduces carbon emissions and maintains forest cover extent. Contrasted with FPInt, by 2020 FPSec yielded 11% greater forest cover with 13% lower net carbon emissions. Forest protection depends on effective prevention of wildfire, logging, and agriculture on forested lands within oil palm leases and PAs.

**Oil Palm Expansion onto Communities' Lands.** In contrast, the BAU trajectory, with ~40% of non-PA land area planted to oil palm by 2020 and only 24% residual forest cover, generates extreme concentration of palm oil agribusiness, with global markets and industry behavior affecting smallholder farmers, local ecosystems, and regional economies. Impacts of such teleconnections are amplified when community-managed lands are converted to plantations. Whereas forests were the primary land cover source (49%) for oil palm across our time series, from 2001 to 2008 agroforests and agricultural fallows comprised the majority (55%) of plantation land clearing. In all future scenarios, even when a 2-km buffer around settlements was enforced (a restriction not required by any current GOI regulations), 28–36% of non-PA lands <5 km from village centers were projected for conversion to oil palm by 2020.

Community-managed agricultural lands are often viewed as underused and treated as "degraded" by governments and companies (8, 9). Moreover, these lands have been recommended as targets for land swaps that aim to shift oil palm from forests (e.g., refs. 5, 44, and 45). However, the term degraded is inherently value laden: Degraded for whom, for how long, and relative to what? Moreover, land sparing worldwide has occurred only under a limited set of circumstances (46). Secondary effects of plantation expansion into established agricultural lands, including smallholder displacement and changes in land access, require long-term assessments of complex responses and impacts (2, 4, 47). Converting swidden agricultural systems disregards both the rights of smallholder farmers and the diverse services these lands provide and may not spare forested lands from deforestation.

**C Sequestration.** Our land change model contributes an advance in carbon accounting by incorporating dynamic forest and agricultural regrowth to estimate carbon emissions offsets. Results suggest that secondary forest, agroforest, and oil palm growth contributed relatively low carbon offsets through sequestration (8% through 2008 and 17% in the BAU scenario). Although carbon sequestered through forest regrowth could become increasingly important in systems experiencing forest transitions over extradecadal timescales (48), we find that reducing proximate carbon emissions requires considerable efforts to achieve continuous protection of existing forests within oil palm leases and PAs.

**Implications.** Protecting intact, logged, and secondary forests but especially peatlands is most critical for reducing carbon emissions from land cover change in Kalimantan. We caution that viable land management solutions—constrained by extensive allocated oil palm leases—may not simultaneously provide full carbon emissions mitigation benefits while protecting smallholder agriculture and maximizing palm oil production. Nevertheless, our analyses generate several insights for evaluating the relative impacts of oil palm plantation development. First, although multiple studies examine trade-offs among future land cover scenarios, rarely have local communities been considered in land policy evaluations (but see ref. 49). Including diverse agents (e.g., communities, governments, and companies) into locally informed and realistic policy simulations will best capture heterogeneous responses to and outcomes from projected conditions. Second, substantially enhanced government and private sector transparency, especially surrounding lease allocation, is critical for understanding the lags and feedbacks that characterize industrial agricultural development (36). Most importantly, assessments of sustainable palm oil must consider land use histories and evaluate whether the process of land acquisition—especially from resident smallholder farmers and communities—not only meets criteria for free, prior, and informed consent or dissent, but also is equitably and transparently compensated. By incorporating diverse trade-offs for multiple agents, such research enhances our capacity to discern context-specific conditions, land use policies, and potential outcomes driven by land acquisition and conversion to plantation agriculture.

## Methods

**Satellite Image Processing.** Eleven Landsat images [thematic mapper (TM) and enhanced thematic mapper plus (ETM+), 30 m; path 121/row 61] were acquired from 1989 to 2008. All were somewhat cloudy (11–71%), so scenes from adjacent years (e.g., 1999 and 2001) were merged to create a time series of 7 images (1–7 y between time steps). Total land area assessed was 12,038 $km^2$. PAs comprised 2,779 $km^2$ with the remaining 9,329 $km^2$ outside PAs. One module of Carnegie Landsat Analysis System–Lite (CLASlite) (50) was used to convert Landsat data to reflectance and to apply a probabilistic spectral unmixing model, yielding fractional cover per pixel consisting of photosynthetic vegetation, nonphotosynthetic vegetation, and soil (50).

**Land Cover Classification.** We developed a land cover classification system using CLASlite and ancillary (e.g., slope) data to identify dominant land covers in the region (Fig. 2 and *SI Methods*). Areas planted with or being cleared for oil palm were manually digitized from Landsat reflectance data, including an image acquired in July 2011. Clearing included roads laid out in gridded patterns indicating future oil palm development. Oil palm locations were confirmed with global positioning system (GPS) data collected from 2005 to 2011.

**Land Change Model.** With Dinamica EGO, we modeled spatially explicit land cover change from 2008 to 2020 (*SI Methods*). We developed a module to allocate oil palm expansion independent of other land cover change. To constrain plantation expansion, we obtained oil palm concession maps ("oil palm leases") for 2008 (*SI Methods*). These leases represent plantations at all stages of the permitting and development process. Over 99% of 2008 planted oil palm fell within these leases, suggesting lease maps provide suitable boundaries for oil palm expansion. Oil palm expansion is a function of plantation establishment rate (i.e., number of leases initiating clearing per annum), annual lease clearing rate, and plantation location. To determine plantation location, plantations initiating clearing were selected randomly from 29 undeveloped oil palm leases. Within an active plantation lease, oil palm expanded until the entire lease area, constrained by specific scenario conditions, was converted. Oil palm could not expand into unsuitable regions (>45° slope, >500 m above sea level) or areas regulated as off-limits (<200 m from rivers, PAs). We collected settlement coordinates (247 villages with >100 households per village) from 2005 to 2010. Oil palm expansion was excluded from circular buffers (2-km radius) around villages.

**Scenarios.** With our model, we contrasted five scenarios of oil palm development. All scenarios were run for 12 y (2008–2020) with ENSO events occurring at 5-y intervals starting from the 2009 ENSO. BAU reflects Indonesia's national objective to double oil palm production by 2020 (40). BAU applies the 2005–2008 mean plantation establishment rate of two plantations initiating clearing per annum and assumes that the area cleared per plantation continues to proceed at the mean 1989–2008 rate (2,900 $ha \cdot y^{-1}$). M scenarios correspond to policies prohibiting forest and peatland conversion to oil palm. The Government of Norway has entered into a bilateral agreement to pay the GOI $1 billion (US) to enforce a mid-2011–2013 moratorium on the allocation of new forestry and plantation permits on "primary natural" forests and peatlands (43). Under the MInt scenario, oil palm plantations initiating clearing from 2012 to 2020 are prohibited from expanding into peatlands and intact (approximately equivalent to primary natural) forests. Our scenario is considerably more restrictive and sustained than the GOI's moratorium; in MInt, expansion is prohibited even if the land was already leased for oil palm in 2008, and restrictions are implemented for 8 y (vs. 2 y under the GOI moratorium). In the MSec scenario, MInt restrictions are expanded to prevent conversion of logged and secondary forests to oil palm. Except for these constraints, the M scenarios are identical to BAU. FP scenarios simulate proposed REDD projects and industry initiatives by

protecting forested lands exempt from oil palm expansion in the M scenarios. Forests in PAs, undeveloped oil palm leases, and oil palm leases initiating clearing post-2011 receive full protection from degradation and deforestation, including fire, from 2012 to 2020. Forests outside oil palm leases and PAs remain unprotected. These protections are implemented in combination with the moratorium on oil palm expansion into intact forests and peatlands. Under the FPInt scenario, intact forests and peatlands are protected from deforestation and logging. The FPSec scenario extends protection to logged and secondary forests. Displaced land cover change or "leakage" may occur when forested lands are protected. In FP simulations, we prevented leakage by protecting forests after allocation of land cover changes for each modeled time step.

**Carbon Flux Quantification.** We designed a carbon bookkeeping model, parameterized with regional carbon data and coupled with the Dinamica EGO land cover change model, to track spatially explicit carbon stocks and flows (*SI Methods*). In the AGB pool (Table S2), we estimated carbon emissions from deforestation and logging of intact, secondary, and logged forests, as well as from agroforest clearing. We measured carbon sequestration from growth of secondary forest, agroforest, and oil palm. In the belowground carbon pool (Tables S3 and S4) we assessed carbon emissions from peatland draining and burning. To estimate emissions from peat draining, land cover classes on peatlands including agroforests, oil palm, burned/cleared, and bare soil were treated as drained. We assumed that no burning occurs in peatlands planted with oil palm and we did not include peat emissions from draining post-2020. Thus, carbon emissions from oil palm on peatlands were underestimated (22).

**ACKNOWLEDGMENTS.** We thank A. Rohman, N. Lisnawati, R. Hartono, Ruspita, W. I. Suci, and Y. Purwanto for invaluable field support; A. Doolittle, P. Raymond, E. Lambin, J. Luzar, and G. Paoli for manuscript feedback; the Indonesian Ministry of Research and Technology and Institute of Sciences for research sponsorship; and the National Science Foundation and National Aeronautics and Space Administration for student fellowships. L.M.C. thanks the following for project financial support: National Aeronautics and Space Administration Land Cover/Land-Use Change Program (NNG05GB51G, NNX11AF08G, and NNX07AK37H), East-West Center, Santa Fe Institute, the John D. and Catherine T. MacArthur Foundation, and Yale and Stanford Universities.

1. Fargione J, Hill J, Tilman D, Polasky S, Hawthorne P (2008) Land clearing and the biofuel carbon debt. *Science* 319:1235–1238.
2. Rudel TK, et al. (2009) Agricultural intensification and changes in cultivated areas, 1970-2005. *Proc Natl Acad Sci USA* 106:20675–20680.
3. Ziegler AD, Fox JM, Xu JC (2009) Agriculture. The rubber juggernaut. *Science* 324: 1024–1025.
4. Lambin EF, Meyfroidt P (2011) Global land use change, economic globalization, and the looming land scarcity. *Proc Natl Acad Sci USA* 108:3465–3472.
5. DeFries R, Rosenzweig C (2010) Toward a whole-landscape approach for sustainable land use in the tropics. *Proc Natl Acad Sci USA* 107:19627–19632.
6. Foley JA, et al. (2011) Solutions for a cultivated planet. *Nature* 478:337–342.
7. van der Werf GR, et al. (2009) $CO_2$ emissions from forest loss. *Nat Geosci* 2:737–738.
8. Fox J, et al. (2009) Policies, political-economy, and swidden in Southeast Asia. *Hum Ecol Interdiscip J* 37:305–322.
9. Mertz O, et al. (2009) Swidden change in Southeast Asia: Understanding causes and consequences. *Hum Ecol Interdiscip J* 37:259–264.
10. Tilman D, Balzer C, Hill J, Befort BL (2011) Global food demand and the sustainable intensification of agriculture. *Proc Natl Acad Sci USA* 108:20260–20264.
11. Lambin EF, Geist HJ (2006) *Land-Use and Land-Cover Change: Local Processes and Global Impacts* (Springer, Berlin), pp 1–222.
12. Curran LM, et al. (1999) Impact of El Niño and logging on canopy tree recruitment in Borneo. *Science* 286:2184–2188.
13. Asner GP, et al. (2006) Condition and fate of logged forests in the Brazilian Amazon. *Proc Natl Acad Sci USA* 103:12947–12950.
14. Curran LM, et al. (2004) Lowland forest loss in protected areas of Indonesian Borneo. *Science* 303:1000–1003.
15. Curran LM, Trigg SN (2006) Sustainability science from space: Quantifying forest disturbance and land-use dynamics in the Amazon. *Proc Natl Acad Sci USA* 103: 12663–12664.
16. Ministry of Agriculture (2010) *Area and Production by Category of Producers: Oil Palm, 1967-2010* (Indonesian Ministry of Agriculture, Jakarta, Indonesia).
17. PricewaterhouseCoopers Indonesia (2010) *Palm Oil Plantation: Industry Landscape, Regulatory and Financial Overview* (PricewaterhouseCoopers Indonesia, Jakarta, Indonesia), pp 1–16.
18. Hansen MC, et al. (2009) Quantifying changes in the rates of forest clearing in Indonesia from 1990 to 2005 using remotely sensed data sets. *Environ Res Lett* 4: 034001.
19. Ministry of Environment (2010) *Second National Communications Report to the UNFCCC* (Indonesian Ministry of Environment, Jakarta, Indonesia), pp 53–84.
20. Gibbs HK, et al. (2010) Tropical forests were the primary sources of new agricultural land in the 1980s and 1990s. *Proc Natl Acad Sci USA* 107:16732–16737.
21. Koh LP, Miettinen J, Liew SC, Ghazoul J (2011) Remotely sensed evidence of tropical peatland conversion to oil palm. *Proc Natl Acad Sci USA* 108:5127–5132.
22. Paoli GD, et al. (2011) Policy perils of ignoring uncertainty in oil palm research. *Proc Natl Acad Sci USA* 108:E218–E218, author reply E219.
23. Langner A, Miettinen J, Siegert F (2007) Land cover change 2002-2005 in Borneo and the role of fire derived from MODIS imagery. *Glob Change Biol* 13:2329–2340.
24. Asner GP (2009) Tropical forest carbon assessment: Integrating satellite and airborne mapping approaches. *Environ Res Lett* 4:034009.
25. Asner GP, et al. (2010) High-resolution forest carbon stocks and emissions in the Amazon. *Proc Natl Acad Sci USA* 107:16738–16742.
26. Morel AC, et al. (2011) Estimating aboveground biomass in forest and oil palm plantation in Sabah, Malaysian Borneo using ALOS PALSAR data. *For Ecol Manage* 262:1786–1798.
27. Ballhorn U, Siegert F, Mason M, Limin S (2009) Derivation of burn scar depths and estimation of carbon emissions with LIDAR in Indonesian peatlands. *Proc Natl Acad Sci USA* 106:21213–21218.
28. Houghton RA (2005) Aboveground forest biomass and the global carbon balance. *Glob Change Biol* 11:945–958.
29. Ramankutty N, Gibbs HK, Achard F, DeFries R, Foley JA (2007) Challenges to estimating carbon emissions from tropical deforestation. *Glob Change Biol* 13:51–66.
30. Uriarte M, Schneider L, Rudel TK (2010) Synthesis: Land transitions in the tropics. *Biotropica* 42:59–62.
31. Miettinen J, Shi CH, Liew SC (2011) Deforestation rates in insular Southeast Asia between 2000 and 2010. *Glob Change Biol* 17:2261–2270.
32. Asner GP, et al. (2005) Selective logging in the Brazilian Amazon. *Science* 310: 480–482.
33. Lawrence D, Peart DR, Leighton M (1998) The impact of shifting cultivation on a rainforest landscape in West Kalimantan: Spatial and temporal dynamics. *Landscape Ecol* 13:135–148.
34. Lawrence D (2005) Biomass accumulation after 10-200 years of shifting cultivation in Bornean rain forest. *Ecology* 86:26–33.
35. Lawrence D, Radel C, Tully K, Schmook B, Schneider L (2010) Untangling a decline in tropical forest resilience: Constraints on the sustainability of shifting cultivation across the globe. *Biotropica* 42:21–30.
36. Murdiyarso D, Dewi S, Lawrence D, Seymour F (2011) *Indonesia's Forest Moratorium: A Stepping Stone to Better Forest Governance?* (Center for International Forestry Research, Bogor, Indonesia).
37. Page SE, Rieley JO, Banks CJ (2011) Global and regional importance of the tropical peatland carbon pool. *Glob Change Biol* 17:798–818.
38. Couwenberg J, Dommain R, Joosten H (2010) Greenhouse gas fluxes from tropical peatlands in south-east Asia. *Glob Change Biol* 16:1715–1732.
39. Murdiyarso D, Hergoualc'h K, Verchot LV (2010) Opportunities for reducing greenhouse gas emissions in tropical peatlands. *Proc Natl Acad Sci USA* 107:19655–19660.
40. Suparno R, Afrida N (December 3, 2009) RI to expand oil palm estates amid environmental concerns. *Jakarta Post.* Available at www.thejakartapost.com/news/2009/12/03/ri-expand-oil-palm-estates-amid-environmental-concerns.
41. Ministry of National Development Planning (2011) *PERPRES No. 61/2011, National Greenhouse Gas Emission Reduction Action Plan* (Indonesian Ministry of National Development Planning, Jakarta, Indonesia), pp 1–153.
42. Soares-Filho BS, et al. (2006) Modelling conservation in the Amazon basin. *Nature* 440:520–523.
43. President of the Republic of Indonesia (2011) INPRES No. 10/2011, Suspension of granting new licenses and improvement of natural primary forest and peatland governance (Republic of Indonesia, Jakarta, Indonesia), pp 1–7.
44. Roundtable on Sustainable Palm Oil (2009) *National Interpretation of RSPO Principles and Criteria for Sustainable Palm Oil Production* (RSPO Indonesian National Interpretation Working Group, Jakarta, Indonesia), pp 1–33.
45. Koh LP, Ghazoul J (2010) Spatially explicit scenario analysis for reconciling agricultural expansion, forest protection, and carbon conservation in Indonesia. *Proc Natl Acad Sci USA* 107:11140–11144.
46. Perfecto I, Vandermeer J (2010) The agroecological matrix as alternative to the land-sparing/agriculture intensification model. *Proc Natl Acad Sci USA* 107:5786–5791.
47. Coomes OT, Takasaki Y, Rhemtulla JM (2011) Land-use poverty traps identified in shifting cultivation systems shape long-term tropical forest cover. *Proc Natl Acad Sci USA* 108:13925–13930.
48. Rudel TK, et al. (2005) Forest transitions: Towards a global understanding of land use change. *Glob Environ Change* 15:23–31.
49. Kremen C, et al. (2000) Economic incentives for rain forest conservation across scales. *Science* 288:1828–1832.
50. Asner GP, Knapp DE, Balaji A, Páez-Acosta G (2009) Automated mapping of tropical deforestation and forest degradation: CLASlite. *J Appl Remote Sens* 3:033543.
51. Soares-Filho BS, Rodrigues HO, Costa WLS (2009) *Modeling Environmental Dynamics with Dinamica EGO* (Universidade Federal de Minas Gerais, Belo Horizonte, Brazil), pp 1–115.

# Supporting Information

## Carlson et al. 10.1073/pnas.1200452109

### SI Methods

**Study Region.** The Ketapang District study region (2°S 110°E) in West Kalimantan spans 0–665 m above sea level (asl). This aseasonal, ever-wet tropical moist forest region receives ~4,125 mm·y$^{-1}$ precipitation (1). During El Niño Southern Oscillation (ENSO)-associated droughts monthly rainfall may decline below 100 mm for 2–5 consecutive months (2, 3). Regional Indonesian residents span diverse ethnicities (e.g., Dayak, Melayu), including government-sponsored transmigrants (4). Population density (16 people·km$^{-2}$ in 2000) is heterogeneous and concentrated in coastal towns (5). This region contains Gunung Palung National Park (GPNP, 1,000 km$^2$) and 1,800 km$^2$ of other protected areas (PAs).

**Land Cover.** Forest vegetation formations in Ketapang include lowland dipterocarp forest, freshwater swamp, heath forest, and peat swamp forest (6); 50% of the study area is classified as peatland (7). Most forests outside PAs have been logged, as industrial logging began in the 1970s (2, 8, 9). In 2002, when the majority of timber concessions ceased operations, oil palm rapidly became the primary commercial land use across West Kalimantan, concentrated particularly in Ketapang, where oil palm plantation development began in the early 1990s.

Throughout this region, rural agrarian communities maintain extensive agroforests and agricultural fallows (collectively referred to as "agroforests"), consisting of small (1–5 ha) parcels including rain-fed rice fields, secondary forest fallows, cash crops (e.g., rattan), rubber (*Hevea brasiliensis*) gardens, and fruit gardens (10). These mosaics often meet Indonesia's national definition of forest, including canopy cover >30%, vegetation height >5 m, and area >0.25 ha (11).

Burned/cleared lands compose a significant regional land cover type. Unplanned fires escaping from plantations and roads are common, especially during ENSO-related droughts (12, 13). Until recently, oil palm companies used fire to prepare forested areas for plantations, despite regulations prohibiting such practices (12, 13). In addition, agrarian households typically burn small (0.5–2 ha) parcels annually to prepare for rain-fed rice cultivation (14).

**Land Cover Classification.** A land cover mapping algorithm was developed using image segmentation and nearest-neighbor classification with eCognition software (15). Inputs to the classification included Carnegie Landsat Analysis System–Lite (CLASlite) data (16), slope and aspect layers, and planted oil palm. Slope and aspect were derived from a 90-m Shuttle Radar Topography Mission (SRTM) Digital Elevation Model (DEM) (17) and resampled to 30 m in ENVI 4.7 (18). To distinguish clearing and degradation of "natural" forests from dynamics associated with swidden agriculture (19–21), we manually delineated forest areas from Landsat reflectance imagery. Slope and aspect data were used to adapt the nearest-neighbor algorithm to correctly classify relatively bright or dark pixels on slopes.

The final classification decision tree in eCognition comprised eight steps: (*i*) multiresolution segmentation to break the image into small segments; (*ii*) spectral difference segmentation to merge spectrally similar segments; (*iii*) classification of oil palm plantations based on manually defined oil palm; (*iv*) nearest-neighbor classification of forest, agriculture, bare soil, and burned/cleared areas based on user-selected samples; (*v*) reclassification of forested areas previously misclassified as agriculture on the basis of the manually defined forest layer; (*vi*) reclassification of forest areas <45 ha to agriculture; (*vii*) nearest-neighbor classification refinement of forest areas into subclasses—intact, logged, and regrowth postlogging—from user-selected samples; and (*viii*) nearest-neighbor classification partitioning agricultural areas on mineral soils into age classes (<10 y and ≥10 y postland clearing) on the basis of user-selected samples.

Because spectral characteristics of peatland forest are distinct from those of forests on mineral soils, peatlands and mineral soils were classified separately. Moreover, because CLASlite's atmospheric correction algorithm does not remove all noise from Landsat images, each image was classified on the basis of samples selected only from that image date. As a result, each set of classification parameters differed slightly.

Nine land cover classes were produced from the classification: (*i*) intact forest; (*ii*) low-intensity logged forest; (*iii*) high-intensity logged forest; (*iv*) secondary forest, defined as recovering logged forests; (*v*) <10 y agroforests and agricultural fallows; (*vi*) ≥10 y agroforests and agricultural fallows; (*vii*) burned or cleared regions; (*viii*) bare soil or built areas; and (*ix*) oil palm plantations. Because all images were somewhat cloudy (11–71%), scenes from adjacent years (e.g., 1999 and 2001) were merged to create a final time series of seven images, at 1- to 7-y intervals, resampled to 100 m. We then applied postclassification change detection to track the history of each pixel, identifying impossible transitions that could not occur during the time interval assessed. For example, transitions from "logged forest" to "intact forest" were reclassified as "secondary forest."

**Validation of Land Cover Classification.** We validated classified land cover maps by visually interpreting high-resolution (0.6 m$^2$) Quickbird imagery and identifying points falling into one of the nine land cover classes. These points were selectively chosen on the basis of extensive global positioning system (GPS) land cover ground truth data collected in 2007–2008 and overlaid on Quickbird imagery in ArcGIS.

We generated confusion matrices to calculate the overall accuracy (*po*), the proportion of the total number of predictions that were correct, and the more conservative kappa coefficient (*k*), which takes into account agreement occurring by chance (22, 23). On mineral soils, comparison between the 2007 classified Landsat image and points ($n$ = 271 points) selected from 2007 Quickbird imagery (~640 km$^2$, July 1 and Oct 17, 2007) yielded $po$ = 0.63 and $k$ = 0.57. On peat soils, comparison between the 2008 classified Landsat image and points ($n$ = 110) selected from 2009 Quickbird imagery (~220 km$^2$, July 9, 2009) yielded $po$ = 0.78 and $k$ = 0.72.

**Analysis of Land Cover.** For presentation of land cover and carbon flux results, low- and high-intensity logging land cover classes and burned/cleared and bare soil/built classes were clumped into single classes ("logging" and "burned/cleared and bare"). However, they were treated as separate classes in the land cover change and carbon bookkeeping models.

**Oil Palm Lease Records and Planting Lag Analysis.** To assess the process of oil palm development, we obtained provincial West Kalimantan oil palm concession maps ("oil palm leases") for 2008 (24). We compiled regional government data on lease allocation from 2004 to 2011 (25–30). To analyze latency between the initiation of lease allocation and planting, we calculated the number of years between the first official record of lease request ("Informasi Lahan") and land clearing recorded from Landsat data. We were able to obtain these data for 14 of the 16 companies with active clearing and planting by 2008.

**Geographic Information Systems (GIS) Data.** Beyond oil palm lease records, our analysis included a variety of spatial datasets. Peatland coverage generated by RePPProT was modified to reflect validated peatland within the study area (7). Protected areas were compiled from the West Kalimantan spatial plan [Rencana Tata Ruang Wilayah Propinsi (RTRWP)] (31) and were supplemented with "designated protected areas" from the World Database of Protected Areas (32) and a map provided by the Gunung Palung National Park Office. Administrative boundaries were derived from the 2003 Potensi Desa economic survey (33).

**Carbon Bookkeeping Model.** A carbon (C) bookkeeping model implemented in Dinamica EGO accounted for changes in aboveground live biomass (AGB) ($tC{\cdot}ha^{-1}$) and peat soil organic carbon (PSOC) ($tC{\cdot}ha^{-1}$). Net carbon flux from time t1 to time t2 was calculated as follows, with positive values indicating net carbon emissions and negative values representing net carbon sequestration:

$$F_{AGB} = (AGB_{t1} - AGB_{t2}) \quad \textbf{[S1]}$$

$$F_{PSOC} = (PSOC_{t1} - PSOC_{t2}) \quad \textbf{[S2]}$$

$$F_{TOTAL} = F_{AGB} + F_{PSOC}. \quad \textbf{[S3]}$$

$F$ is net C flux ($tC{\cdot}ha^{-1}$), AGB is AGB of land cover ($tC{\cdot}ha^{-1}$), and PSOC is peat soil organic C ($tC{\cdot}ha^{-1}$).

Net carbon flux from land cover change has been quantified using two distinct approaches (34). First, an annual balance calculation considers the balance of carbon entering and leaving the system each year and is the method required under the Kyoto Protocol. Second, a net committed emissions method accounts for the net carbon flux as a system enters a new equilibrium following a shift in land cover. Here, we assumed that all AGB pool carbon is emitted during the year of burning or clearing, but calculated soil carbon flux and sequestration from forest regrowth annually. Thus, we used a hybrid annual balance/net committed emissions approach.

Our carbon bookkeeping model attributed carbon flux only to detectable land cover transitions. For example, if an intact forest pixel was cleared for oil palm, emissions generated from clearing intact forest were ascribed to oil palm. However, if the same intact forest pixel was logged at time $t$ and cleared for oil palm at time $t + 1$, only carbon lost from clearing logged forest was ascribed to oil palm.

**Aboveground Live Biomass.** We quantified AGB stocks on the basis of a combination of land cover (i.e., intact forest, logged forest, secondary forest, agroforest, oil palm, burned/cleared, bare), elevation (i.e., ≤300 m asl, >300 m asl), soil type (i.e., peat or mineral soils), and land cover age. We used a standard carbon fraction (0.5) to convert dry biomass to C (35). Unless otherwise noted, error is reported as ±1 SD. Initial AGB inputs were iteratively modified on the basis of observed land cover transitions (Table S2).

***Intact forests.*** Because forest AGB generally declines with increasing elevation, we partitioned mineral soil forests into two altitudinal classes: ≤300 m asl (lowland) and >300 m asl (upland) (3, 36). For lowland forests, we used published AGB estimates collected in the Ketapang study region from alluvial soils (401 ± 146 $tC{\cdot}ha^{-1}$); for upland forests, we used estimates from granitic soils (292 ± 101 $tC{\cdot}ha^{-1}$) (1). For intact peatland forests, we used AGB estimates (180 ± 108 $tC{\cdot}ha^{-1}$) from Sumatra and Kalimantan (37, 38), compiled by Murdiyarso et al. (39).

Both net carbon sequestration and net carbon emissions have been measured in forests without recent history of anthropogenic disturbance (40–42). In Ketapang, intact forests were estimated to be sequestering carbon at ∼1.76% $AGB{\cdot}y^{-1}$ (1). However, disturbance rate and magnitude limit biomass accumulation at the forest stand level; our land cover change model, by incorporating forest degradation, accounts for such changes. Given the lack of consensus on intact forest carbon dynamics, as well as the inclusion of forest disturbance and regrowth dynamics in our land cover change model, we applied 0% aboveground biomass increment (ABI) ($tC{\cdot}ha^{-1}{\cdot}y^{-1}$) for intact forests.

***Logged forests.*** To account for the influence of initial AGB on postdisturbance AGB, we calculated AGB loss from logging as the fraction of predisturbance forest biomass (43, 44). No distinction was made according to substrate; mineral and peatland forests were assigned identical proportions of AGB loss. Much forest degradation in Kalimantan is due to mechanized logging and to a lesser extent to understory forest fires and "illegal" logging (2, 9, 45, 46). We used AGB losses measured in mechanically logged forests to represent heavy logging and losses measured in illegally logged forests to represent low-intensity logging.

To estimate biomass in "low-intensity logged" forests, in 2007–2008 we measured AGB in Gunung Tarak Protected Forest (*Hutan Lindung*), a region with active illegal logging during that period. We measured DBH and height of all trees ≥10 cm diameter at breast height (DBH) in 153 circular plots with 15-m radius (11-ha sample), covering ∼16 $km^2$ in both 2007 and 2008. In 2007, 9 plots had no evidence of logging (no commercial size stumps >29 cm DBH), but incurred logging activity before the 2008 remeasurement. To calculate the biomass lost from these 9 plots, we applied a moist forest allometric equation (47), incorporating height (meters), DBH (centimeters), and wood-specific gravity ($g/cm^3$). Remaining AGB 1 y after logging averaged 194 ± 116 $tC{\cdot}ha^{-1}$, representing ∼30% loss of AGB from selective nonmechanized illegal logging.

To estimate AGB in "high-intensity logged" forests, we applied biomass measures collected from 1991–1992 in a timber concession in Ketapang District (48). In this commercial concession, remaining biomass 1 y postlogging averaged ∼124 $tC{\cdot}ha^{-1}$, representing ∼41% of AGB before timber harvest. Thus, we applied a 60% biomass loss to high-intensity logged forests, similar to the estimated range of biomass lost from logging reported in studies across Asia (49).

***Secondary forests.*** In regrowing logged forests, ABI is positively related to the basal area of residual trees (43). Postdisturbance biomass recovery may thus be represented as percentage of AGB rather than absolute ABI. The relationship between AGB and ABI is nonlinear, and high mortality during the first few years postdisturbance may offset biomass accumulation (43, 50, 51). However, AGB begins to accumulate as tree mortality in these forests returns to nonanthropogenic rates; in logged forest stands in northeastern Borneo, AGB would require ≥120 y to reach prelogged levels (52). To initiate our carbon bookkeeping model, secondary forests were assigned the same AGB as high-intensity logged forests. To account for carbon sequestration from secondary forest regrowth, we used an annual recovery rate of 1.80 ± 0.93% of AGB, as measured in northern Borneo 18 y after logging (53).

***Agroforests.*** The agroforest land cover class includes land uses as diverse as rubber gardens, wet rice fields, upland dry rice fallows, and coconut groves. Factors such as tree stocking densities, fallow period, and number of farming events influence AGB within each of these subclasses (14, 54, 55). We were unable to account for biomass variations among these classes because spectral and spatial resolution of Landsat imagery cannot discern these often small (∼1 $ha{\cdot}parcel^{-1}$) and spectrally similar patches.

Instead, agroforest AGB was calculated from equations relating AGB with land cover age on the basis of the dynamics of dry rice fallows, one of the dominant managed land covers in this region (10). To develop a relationship between fallow age and AGB, we sampled 31 sites ranging from age 5 y to 39 y in Kembera, a village within the study region (14). Sampling was conducted from 1993 to 1996 in sites concentrated in an area of ∼3 × 3 km. Two sampling regimes were applied. For 24 of the sites a 0.1-ha plot (20 × 50 m)

was randomly located within the fallow. For 7 of the sites, 0.3 ha (four 30 × 25-m plots) was sampled following methods described in Lawrence (14). In each plot, DBH of all trees >10 cm was measured. Stem AGB was calculated as described in Lawrence (14), using relationships developed by Hughes et al. (56) and Brown et al. (57). Linear regression yielded mean and 95% confidence interval relationships between agroforest age and AGB ($n = 31, r^2 = 0.72$). Initially, agroforests were divided into two age classes (young, <10 y; and mature, ≥10 y postclearing) on the basis of their spectral properties. For young agroforests, age was assumed to be zero. All mature agroforests were assigned the lowest age (10 y) in this range, so that initial AGB for these mature agroforests was 22 ± 8 tC·ha$^{-1}$. This assumption potentially underestimates carbon stocks in the agroforest land cover class. However, as the core component of a swidden farming system these mature agroforests are subject to periodic reclearing (e.g., refs. 58 and 59), limiting the total biomass stored in this agroforest mosaic.

***Oil palm.*** Oil palm AGB was estimated from age–biomass equations developed from measurements of 3- to 30-y oil palm in Kalimantan and Sumatra (60, 61). Regression analysis yielded mean and 95% confidence interval relationships between oil palm age and AGB ($n = 15, r^2 = 0.56$).

***Burned and cleared lands.*** Burned/cleared as well as bare soil/built area classes were assigned 0 tC·ha$^{-1}$ AGB.

**Belowground Carbon.** Undisturbed peat soils that maintain acidic and anaerobic conditions are net carbon sinks, but become carbon sources through peatland draining or burning (62–64). Peat soil accumulation rates are estimated at ~0.5–2 mm·y$^{-1}$ in undisturbed organic peat soils (65, 66). Given the relatively brief 32-y period modeled here, carbon sequestration from peat accumulation (0.6–1.2 tC y$^{-1}$) is negligible compared with carbon emissions from peatlands (16 tC y$^{-1}$ in drained peat soils or 203 tC in a single burning event), and thus peat accumulation was excluded from our carbon sequestration estimates. We account only for losses of peat soil organic carbon (tC·ha$^{-1}$) from peat burning and oxidation:

$$\mathrm{PSOC}_{t2} = \mathrm{VCD}\,(D_{t1} - D_{\mathrm{BURN}}) - O\,(t2 - t1). \qquad \textbf{[S4]}$$

PSOC is peat SOC (tC·ha$^{-1}$), VCD is volumetric C density (tC·ha$^{-1}$·m$^{-1}$), $D$ is peat depth (meters), $D_{\mathrm{BURN}}$ is depth of peat burned (meters), and $O$ is emissions from oxidation of drained peat (tC·ha$^{-1}$·y$^{-1}$).

***Peat depth map.*** To estimate peat depth across the study region, we constructed a multiple linear regression model predicting peat depth from Landsat reflectance and elevation data. In 2005, peat depth was measured at 152 points spaced every 1 km across 2 × 23-km transects in the Sungai Putri peat area located within the study region. These measurements generated 4.5 ± 2.3 m mean peat depth. Depth samples were stratified by land cover superclass, forest (i.e., intact, logged, or secondary forest) and nonforest (i.e., agroforest, burned/cleared, or bare soil), in 1989 and 2005. To ensure peat depth did not change as a result of deforestation and drainage, the dataset was subset to samples remaining in the same superclass in both years ($n = 117$). Using peat depth as the dependent variable and 1989 Landsat reflectance bands (1–5, 7) and elevation (meters asl) as independent variables, we tested linear combinations of these variables to predict peat depth. The model best estimating peat depth ($n = 117, r^2 = 0.53$) is:

$$0.287 + (0.0102)\,\mathrm{B2} + (-0.00436)\,\mathrm{B5} + (0.217)\,E. \qquad \textbf{[S5]}$$

B2 is Landsat reflectance band 2, B5 is Landsat reflectance band 5, and $E$ is elevation.

We applied this model to the 1989 reflectance image, constraining peat depth to 0–10 m and using Delaunay triangulation in ENVI 4.7 to fill no-data pixels occurring within peat areas (18). Peat depth maps were used to account for residual carbon stocks in organic peat soils; when burn depth or decrement due to carbon emissions from peat draining exceeded peat depth, a pixel was assigned a depth of zero and was no longer able to emit carbon from burning or draining.

***Peat soils—volumetric carbon density calculation.*** Volumetric peat carbon density is the product of bulk density (BD) (t·m$^{-3}$) and peat carbon content (CC) (%). In intact peat forests, BD and CC vary spatially with peatland type, yet display a relatively narrow range of values throughout the Indonesian archipelago (63, 67–69). Nonforest lands may have elevated BD due to compaction (70); yet for this study we assume equivalent volumetric peat carbon density across all land cover classes. We parameterize our assessments with data collected in Kalimantan and Sumatra, compiled by Shimada et al. (68). These measurements ($n = 6$ forest types) yield a CC of 55.93 ± 1.79%, with mean bulk density of 0.110 ± 0.021 t·m$^{-3}$, generating volumetric peat carbon density of 480–757 tC·m$^{-1}$·ha$^{-1}$.

***Peat soils—burning.*** Peat depth loss from burning in Central Kalimantan has been observed at ~0.33 ± 0.18 m (71); emissions are calculated accordingly for burned peat (Table S3) (68).

***Peat soils—draining.*** Peat soil emissions increase with drainage depth, which in turn is determined by land cover (72). However, drainage depth within a single land cover class is variable; thus for all drained peatlands (i.e., agroforests and agricultural fallows, burned/cleared, bare soil, and oil palm), we applied a single carbon emission rate of 15.89 ± 3.07 tC·ha$^{-1}$·y$^{-1}$ calculated from closed-chamber $CO_2$ flux studies in Borneo and Sumatra (Table S4) (38, 64, 73–75). Nonforested peat depth was decremented 2–4 cm·y$^{-1}$, equivalent to the carbon emission rate above, to account for this loss of carbon.

**Carbon Accounting, 1989–2008.** Because of >1-y intervals in the 1989–2008 land cover change model, we made several informed assumptions to assign t1 and t2 for carbon bookkeeping purposes. In the AGB pool, all transitions were initiated at the beginning of the time interval. Peatlands were assumed to burn only once per interval. Peatlands transitioning from "undrained" to "drained" were assumed to be drained halfway through a given interval. For example, in the 2005–2007 interval, peatlands transitioning from intact forest in 2005 to oil palm in 2007, emissions from the peat draining pool accrued starting in 2006. Because initial oil palm development in the study region occurred in 1994, draining emissions for undrained peatlands transitioning to oil palm from 1989 to 1996 were initiated in 1994. For the future carbon bookkeeping model, all land cover change and commensurate carbon emissions were assumed to occur at the beginning of an annual interval.

**Land Cover Change Model.** We modeled land cover change in Dinamica EGO, an environmental modeling platform that allows spatially explicit simulation of landscape dynamics (76). Our model incorporates oil palm expansion as well as non oil palm land cover change.

***Land cover change 1989–2008.*** In the historic land cover change model, two dynamic spatial model inputs were used: cell age and peat depth. Three static spatial model inputs were applied: classified land cover, elevation, and distance to village. For carbon accounting purposes, all land cover ages were initially zero, except ≥10-y agricultural fallows, conservatively assigned the lowest age (10 y). In 1989 at the onset of remote sensing analysis, no oil palm plantations were present, so initial oil palm age estimation was unnecessary. On the basis of land cover transitions observed between successive images, for each image date the model calculated (*i*) land cover age, (*ii*) peat depth, (*iii*) aboveground and belowground carbon stocks, (*iv*) cell age, and (*v*) carbon flux from each carbon pool.

***Future land cover change 2008–2020.*** Dinamica EGO uses a Bayesian weights-of-evidence (WOFE) method to derive spatial proba-

bilities identifying the most likely areas for land cover transitions (76). Transition matrices specify the proportion of cells that change from one class to another per time step. Then, a local cellular automaton, comprised of customizable Expander and Patcher functions, expands, contracts, or forms new patches of a given land cover class according to cell transition probabilities.

Because ENSO events precipitate drought and late onset of rains in Borneo, facilitating fires and commensurate deforestation with associated carbon emissions (12, 77), we derived transition matrices from the 1996–1997 period to represent ENSO years and the 2007–2008 period to represent non-ENSO years. Climate records indicate that ENSO events occur every 2–7 y, with a recent periodicity of 5.3 y (78, 79). Our model applied ENSO transition matrices every 5 y starting with the 2009 ENSO event (i.e., 2009, 2014, 2019); other years used non-ENSO transition matrices.

Land cover transitions were constrained so that all forest-to-agroforest transitions passed through a burning/clearing stage. Agroforests were prevented from recovering to become natural forests. Transition matrices and WOFE were derived separately for mineral soil and peatland regions. All land cover change was modeled from transition rates and WOFE except oil palm plantation expansion.

***Oil palm expansion.*** Predicting plantation establishment rate and location is difficult. Diverse sociopolitical and economic factors alter the opportunity cost of land use, onset of plantation operations, and rate of company clearing and planting. Developers wishing to acquire land for plantation agriculture in Indonesia must follow a complex process potentially including approaching the Bupati and/or provincial Governor, an environmental impact assessment, rezoning of land in the forest estate, negotiations with local communities, and concession boundary surveys. These steps must be completed before a 25-y *Hak Guna Usaha* (HGU, cultivation rights) certificate is issued to the developer (80).

***Weights of evidence.*** WOFE are calculated on the basis of the association among land cover transitions and spatial evidence layers (e.g., the relationship between a transition from intact forest to burned/cleared and distance to oil palm) (76, 81). Because WOFE maps are assumed to be spatially independent, we used a suite of statistical measures (e.g., Cramer's contingency coefficient) provided in Dinamica to calculate the correlation between input maps. We discarded highly correlated maps, yielding 11 maps suitable as independent evidence layers. These layers consisted of continuous dynamic (i.e., age, distance to deforestation, distance to logging, distance to nonforest, distance to oil palm, peat depth, and travel cost) continuous static (i.e., distance to towns, elevation, slope), and categorical static (PA) layers. Here, nonforest refers to agroforest, burned/cleared, oil palm, and bare soil classes. For certain land cover transitions, WOFE for layers with no bearing on transition likelihood were removed (e.g., slope was not used in determining the location of peatland transitions because peatlands are located in relatively flat lowland basin drainages). WOFE were derived from the 2007–2008 time step and were calculated separately for mineral soil and peatland regions because of different land cover change dynamics in these two ecotypes.

***Patch geometry calibration.*** Spatial patterns of change in Dinamica EGO are produced with a cellular automaton composed of two transition functions, Expander and Patcher. Each process forms patches in a variety of shapes and sizes on the basis of mean patch size, patch size variance, and patch isometry (82). To calibrate Expander and Patcher, we analyzed the 2007–2008 time step to derive patch size mean and variance for all transitions. We modified transitions to the burned/bare class to simulate the tendency of fire to spread from previously burned areas (mean burned/bare patch size 10 ha in the Expander function) and also augmented new burned/bare patch mean area and variance (mean burned/bare patch size 1–5 ha in the Patcher function). These values were used to calibrate Patcher and Expander transition parameters. Patch isometry, which ranges from 0 to 2 with higher values being more isometric, was set to 1.0 for all transitions in both Patcher and Expander. For most transitions, 50% of change was allocated to the Patcher function with the remainder allocated to Expander. For transitions to fire, 70% of change was allocated to the Expander function.

***Travel cost surfaces.*** Travel cost—the economic cost of moving from one point to another on a landscape—is one of the spatial determinants of land cover change (83, 84). Thus, one of the spatial layers used to derive probability maps in the land cover simulation model was travel cost to regional ports. Travel cost depends on trip length as well as the difficulty, or friction, of traveling that distance; lower friction values indicate less costly travel. Inputs to travel cost calculations were maps of land cover, roads, rivers, and ports. Road maps were developed by digitizing roads from each Landsat image in the time series. Future road maps were simulated using a road-building module in Dinamica EGO, which extends unpaved roads from existing roads into newly planted oil palm areas (85). River maps were created by digitizing rivers visible in Landsat reflectance imagery. We identified coastal ports at major cities (Ketapang and Sukadana) as well as one port on an island (Maya Karimata) as travel destinations. Friction surface maps were created by assigning paved roads and rivers a friction value of 1, nonpaved roads a value of 10, and logging roads a value of 20. Intact forests were assigned a friction value of 500; logged and secondary forests, values of 400; agricultural fallows and cleared/burned areas, values of 200; and oil palm and bare soils areas, values of 100. On the basis of the friction surface maps and port locations, travel cost was calculated in Dinamica EGO using the "Calc Cost Map" function.

***Carbon sensitivity analysis.*** To offer uncertainty bounds on carbon flux from land cover change, we calculated carbon flux using mean, low, and high carbon input values for AGB, carbon emissions from oxidation of drained peat ($tC \cdot ha^{-1}$), peat depth loss due to fire (meters), and peat volumetric carbon density ($tC \cdot ha^{-1} \cdot m^{-1}$). The three (mean, low, and high) carbon scenarios were applied to the historic time series as well as future land cover change scenarios. In the historic land cover results, carbon flux from minimum and maximum carbon inputs is presented as model error, whereas in each scenario, mean, minimum, and maximum values were generated from the mean of 20 model runs with mean, minimum, and maximum input values.

***Land cover change model validation.*** We validated our model by comparing actual change from 2005 to 2007 with modeled change from 2005 to 2007. We excluded transitions to oil palm from these comparisons, as oil palm plantation establishment location within oil palm lease areas is impossible to predict without information garnered from government officials or company representatives. Simulated maps inherit the spatial pattern of the initial landscape map; to control for this effect, we assessed only differences between the two maps. The validation uses a reciprocal fuzzy comparison test, using a decay function to examine how window size ($1 \times 1$ cell or $100 \times 100$ m to $11 \times 11$ cells or $1{,}100 \times 1{,}100$ m) affects fitness (76, 86). Applying a linear decay function in the fuzzy reciprocal validation, fitness increased from 25% at a $1 \times 1$ resolution to 81% at $11 \times 11$ cell resolution. Applying an exponential decay function at an $11 \times 11$ cell resolution generated a mean minimum similarity index of 0.49. Thus, although our model does a poor job of predicting cell-by-cell change, predictive power within the $11 \times 11$ cell neighborhood is high (81%).

**Potential Sources of Uncertainty.** Canopy gaps in disturbed forests rapidly regrow to spectrally resemble nondisturbed forest; thus accurate forest degradation and logging detection requires an annual time series of cloud-free images, unavailable for this region. Although the frequency of image acquisition in this study (1–7 y) detects most forest disturbance, especially for longer intervals between images (e.g., 1989–1996), our measures likely

underestimate secondary forest and as a result overestimate intact forest cover.

Water tables in forested areas may be lowered by nearby draining, road construction, or burning, making such peat forests net sources of carbon to the atmosphere (87). By assuming no emissions from peat forests adjacent to drained peatlands, we underestimate carbon emissions from forested peatlands.

We ascribed emissions from burning only to the burned/cleared land cover class and assumed that no burning occurs in peatlands planted with oil palm. Especially from 1990 to 2000, few oil palm plantation companies complied with regulations prohibiting clearing land with fire (12, 88). Moreover, drained peatland soils planted with oil palm are vulnerable to fire (89). Thus, fire-related carbon emissions from oil palm expansion on peatlands were underestimated.


1. Paoli GD, Curran LM (2007) Soil nutrients limit aboveground productivity in mature lowland tropical forests of Southwestern Borneo. *Ecosystems* 503:503–518.
2. Curran LM, et al. (1999) Impact of El Niño and logging on canopy tree recruitment in Borneo. *Science* 286:2184–2188.
3. Paoli GD, Curran LM, Slik JWF (2008) Soil nutrients affect spatial patterns of aboveground biomass and emergent tree density in southwestern Borneo. *Oecologia* 155:287–299.
4. Fearnside PM (1997) Transmigration in Indonesia: Lessons from its environmental and social impacts. *Environ Manage* 21:553–570.
5. Central Statistics Agency (2000) *Population Census 2000* (Indonesian Central Statistics Agency, Jakarta, Indonesia).
6. Curran LM, Leighton M (2000) Vertebrate responses to spatiotemporal variation in seed production of mast-fruiting dipterocarpaceae. *Ecol Monogr* 70:101–128.
7. Regional Physical Planning Programme for Transmigration (1990) *A National Overview from the Regional Physical Planning Programme for Transmigration*. (UK Overseas Development Administration and Directorate Bina Programme, Ministry of Transmigration, Jakarta, Indonesia).
8. Curran LM, Webb CO (2000) Experimental tests of the spatiotemporal scale of seed predation in mast-fruiting Dipterocarpaceae. *Ecol Monogr* 70:129–148.
9. Curran LM, et al. (2004) Lowland forest loss in protected areas of Indonesian Borneo. *Science* 303:1000–1003.
10. Lawrence D, Peart DR, Leighton M (1998) The impact of shifting cultivation on a rainforest landscape in West Kalimantan: Spatial and temporal dynamics. *Landscape Ecol* 13:135–148.
11. Ministry of Forestry (2004) *Regulation No. P.14/2004 Concerning Rules and Procedures for Implementation of A/R CDM* (Indonesian Ministry of Forestry, Jakarta, Indonesia).
12. Siegert F, Ruecker G, Hinrichs A, Hoffmann AA (2001) Increased damage from fires in logged forests during droughts caused by El Niño. *Nature* 414:437–440.
13. Dennis RA, et al. (2005) Fire, people, and pixels: Linking social science and remote sensing to understand underlying causes and impacts of fires in Indonesia. *Hum Ecol Interdiscip J* 33:465–504.
14. Lawrence D (2005) Biomass accumulation after 10-200 years of shifting cultivation in Bornean rain forest. *Ecology* 86:26–33.
15. Definiens (2009) *Definiens eCognition Developer 8 – User Guide* (Munich).
16. Asner GP, Knapp DE, Balaji A, Páez-Acosta G (2009) Automated mapping of tropical deforestation and forest degradation: CLASlite. *J Appl Remote Sens* 3:033543.
17. Jarvis A, Reuter HI, Nelson A, Guevara E (2006) *Hole-Filled Seamless SRTM Data V3* (CIAT - International Center for Tropical Agriculture, Cali, Columbia).
18. ITT Visual Information Solutions (2009) *ENVI 4.7* (ITT Visual Information Solutions, Boulder, CO).
19. Fox J, Vogler JB (2005) Land-use and land-cover change in montane mainland southeast Asia. *Environ Manage* 36:394–403.
20. DeFries R, et al. (2007) Earth observations for estimating greenhouse gas emissions from deforestation in developing countries. *Environ Sci Policy* 10:385–394.
21. Mertz O, et al. (2009) Swidden change in Southeast Asia: Understanding causes and consequences. *Hum Ecol Interdiscip J* 37:259–264.
22. Cohen J (1960) A coefficient of agreement for nominal scales. *Educ Psychol Meas* 20: 37–46.
23. Congalton RG (1991) A review of assessing the accuracy of classifications of remotely sensed data. *Remote Sens Environ* 37:35–46.
24. West Kalimantan National Land Body (2008) *Distribution of Plantations, Transmigration, Fisheries and Industrial Forest Plantations, West Kalimantan Province* (West Kalimantan National Land Body, Pontianak, Indonesia).
25. West Kalimantan Plantation Agency (2004) *Plantation Land Use Development in West Kalimantan, January 2003* (West Kalimantan Plantation Agency, Pontianak, Indonesia).
26. West Kalimantan Plantation Agency (2005) *Plantation Land Use Development in West Kalimantan, 2004* (West Kalimantan Plantation Agency, Pontianak, Indonesia).
27. Plantation Estate Agency (2006) *List of Oil Palm Company Names in Kabupaten Ketapang Through October 2006* (Ketapang District Plantation Estate Agency, Ketapang, Indonesia).
28. West Kalimantan Plantation Agency (2006) *Plantation License Development in West Kalimantan Through 2nd Semester 2005* (West Kalimantan Plantation Agency, Pontianak, Indonesia).
29. West Kalimantan Plantation Agency (2006) *Plantation License Development in West Kalimantan Through July 2005* (West Kalimantan Plantation Agency, Pontianak, Indonesia).
30. West Kalimantan Plantation Agency (2011) *Plantation License Development in West Kalimantan Through December 2010* (West Kalimantan Plantation Agency, Pontianak, Indonesia).
31. West Kalimantan Provincial Government (2004) *Provincial Spatial Plan, Local Regulation No. 8 Year 2003* (West Kalimantan Provincial Government, Pontianak, Indonesia).
32. International Union for Conservation of Nature and United Nations Environment Program - World Conservation Monitoring Center (2010) The World Database on Protected Areas (WDPA): Annual Release. (United Nations Environment Program - World Conservation Monitoring Center, Cambridge, UK).
33. Central Statistics Agency (2004) Potensi Desa (PODES) 2003. *Agricultural Census 2003: National Total Results of Household Surveys* (Indonesian Central Statistics Agency, Jakarta, Indonesia).
34. Fearnside PM (1997) Greenhouse gases from deforestation in Brazilian Amazonia: Net committed emissions. *Clim Change* 35:321–360.
35. Brown S, Lugo AE (1982) The storage and production of organic-matter in tropical forests and their role in the global carbon-cycle. *Biotropica* 14:161–187.
36. Kitayama K, Aiba S (2002) Ecosystem structure and productivity of tropical rain forests along altitudinal gradients with contrasting soil phosphorus pools on Mount Kinabalu, Borneo. *J Ecol* 90:37–51.
37. Waldes NJL, Page SE (2002) Forest structure and tree diversity of a peat swamp forest in Central Kalimantan, Indonesia. *International Symposium on Tropical Peatlands*, eds Rieley JO, Page SE, Setiadi B (Badan Pengkajian dan Penerapan Teknologi, Jakarta, Indonesia), pp 16–22.
38. Ali M, Taylor D, Inubushi K (2006) Effects of environmental variations on $CO_2$ efflux from a tropical peatland in eastern Sumatra. *Wetlands* 26:612–618.
39. Murdiyarso D, Hergoualc'h K, Verchot LV (2010) Opportunities for reducing greenhouse gas emissions in tropical peatlands. *Proc Natl Acad Sci USA* 107: 19655–19660.
40. Baker TR, et al. (2004) Increasing biomass in Amazonian forest plots. *Philos Trans R Soc Lond B Biol Sci* 359:353–365.
41. Rice AH, Pyle EH, Saleska SR, Hutyra L, Palace M (2004) Carbon balance and vegetation dynamics in an old-growth Amazonian forest. *Ecol Appl* 14:S55–S71.
42. Houghton RA (2007) Balancing the global carbon budget. *Annu Rev Earth Planet Sci* 35:313–347.
43. Mazzei L, et al. (2010) Above-ground biomass dynamics after reduced-impact logging in the Eastern Amazon. *For Ecol Manage* 259:367–373.
44. Sasaki N, et al. (2011) Approaches to classifying and restoring degraded tropical forests for the anticipated REDD+ climate change mitigation mechanism. *iForest* 4: 1–6.
45. Casson A, Obidzinski K (2002) From new order to regional autonomy: Shifting dynamics of "illegal" logging in Kalimantan, Indonesia. *World Dev* 30:2133–2151.
46. Langner A, Miettinen J, Siegert F (2007) Land cover change 2002-2005 in Borneo and the role of fire derived from MODIS imagery. *Glob Change Biol* 13:2329–2340.
47. Chave J, et al. (2005) Tree allometry and improved estimation of carbon stocks and balance in tropical forests. *Oecologia* 145:87–99.
48. Cannon CH, Peart DR, Leighton M, Kartawinata K (1994) The structure of lowland rainforest after selective logging in West Kalimantan, Indonesia. *For Ecol Manage* 67:49–68.
49. Lasco RD (2002) Forest carbon budgets in Southeast Asia following harvesting and land cover change. *Sci China C Life Sci* 45:55–64.
50. Silva JNM, et al. (1995) Growth and yield of a tropical rainforest in the Brazilian Amazon 13 years after logging. *For Ecol Manage* 71:267–274.
51. Sist P, Sheil D, Kartawinata K, Priyadi H (2003) Reduced-impact logging in Indonesian Borneo: Some results confirming the need for new silvicultural prescriptions. *For Ecol Manage* 179:415–427.
52. Pinard MA, Cropper WP (2000) Simulated effects of logging on carbon storage in dipterocarp forest. *J Appl Ecol* 37:267–283.
53. Berry NJ, et al. (2010) The high value of logged tropical forests: Lessons from northern Borneo. *Biodivers Conserv* 19:985–997.
54. Salafsky N (1994) Forest gardens in the Gunung Palung region of West Kalimantan, Indonesia: Defining a locally-developed, market-oriented agroforestry system. *Agrofor Syst* 28:237–268.
55. Ketterings QM, Coe R, van Noordwijk M, Ambagau' Y, Palm CA (2001) Reducing uncertainty in the use of allometric biomass equations for predicting above-ground tree biomass in mixed secondary forests. *For Ecol Manage* 146:199–209.
56. Hughes RF, Kauffman JB, Jaramillo VJ (1999) Biomass, carbon, and nutrient dynamics of secondary forests in a humid tropical region of Mexico. *Ecology* 80:1892–1907.
57. Environmental Systems Research Institute (2007) *ArcGIS 9.2* (Environmental Systems Research Institute, Redlands, CA).
58. Mertz O, et al. (2008) A fresh look at shifting cultivation: Fallow length an uncertain indicator of productivity. *Agric Syst* 96:75–84.
59. Lawrence D, Radel C, Tully K, Schmook B, Schneider L (2010) Untangling a decline in tropical forest resilience: Constraints on the sustainability of shifting cultivation across the globe. *Biotropica* 42:21–30.
60. Corley RHV, Tinker PB (2003) *The Oil Palm* (Blackwell, Oxford), 4th Ed, pp 1–592.
61. Syahrinudin (2005) *The Potential of Oil Palm and Forest Plantations for Carbon Sequestration on Degraded Land in Indonesia* (Cuvillier, Gottingen, Germany), pp 1–115.
62. Armentano TV, Menges ES (1986) Patterns of change in the carbon balance of organic soil-wetlands of the temperate zone. *J Ecol* 74:755–774.
63. Page SE, et al. (2002) The amount of carbon released from peat and forest fires in Indonesia during 1997. *Nature* 420:61–65.
64. Furukawa Y, Inubushi K, Ali M, Itang AM, Tsuruta H (2005) Effect of changing groundwater levels caused by land-use changes on greenhouse gas fluxes from tropical peat lands. *Nutr Cycl Agroecosyst* 71:81–91.

65. Page SE, et al. (2004) A record of Late Pleistocene and Holocene carbon accumulation and climate change from an equatorial peat bog (Kalimantan, Indonesia): Implications for past, present and future carbon dynamics. *J Quat Sci* 19:625–635.
66. Dommain R, Couwenberg J, Joosten H (2011) Development and carbon sequestration of tropical peat domes in south-east Asia: Links to post-glacial sea-level changes and Holocene climate variability. *Quat Sci Rev* 30:999–1010.
67. Sorensen KW (1993) Indonesian peat swamp forests and their role as a carbon sink. *Chemosphere* 27:1065–1082.
68. Shimada S, Takahashi H, Haraguchi A, Kaneko M (2001) The carbon content characteristics of tropical peats in Central Kalimantan, Indonesia: Estimating their spatial variability in density. *Biogeochemistry* 53:249–267.
69. Jauhiainen J, Takahashi H, Heikkinen JEP, Martikainen PJ, Vasander H (2005) Carbon fluxes from a tropical peat swamp forest floor. *Glob Change Biol* 11:1788–1797.
70. Kool DM, Buurman P, Hoekman DH (2006) Oxidation and compaction of a collapsed peat dome in Central Kalimantan. *Geoderma* 137:217–225.
71. Ballhorn U, Siegert F, Mason M, Limin S (2009) Derivation of burn scar depths and estimation of carbon emissions with LIDAR in Indonesian peatlands. *Proc Natl Acad Sci USA* 106:21213–21218.
72. Hooijer A, et al. (2009) Current and future $CO_2$ emissions from drained peatlands in Southeast Asia. *Biogeosci Discuss* 6:7207–7230.
73. Inubushi K, Furukawa Y, Hadi A, Purnomo E, Tsuruta H (2003) Seasonal changes of $CO(_2)$, $CH(_4)$ and $N(_2)O$ fluxes in relation to land-use change in tropical peatlands located in coastal area of South Kalimantan. *Chemosphere* 52:603–608.
74. Hadi A, et al. (2005) Greenhouse gas emissions from tropical peatlands of Kalimantan, Indonesia. *Nutr Cycl Agroecosyst* 71:73–80.
75. Melling L, Hatano R, Goh KJ (2005) Soil $CO_2$ flux from three ecosystems in tropical peatland of Sarawak, Malaysia. *Tellus B Chem Phys Meterol* 57B:1–11.
76. Soares-Filho BS, Rodrigues HO, Costa WLS (2009) *Modeling Environmental Dynamics with Dinamica EGO* (Universidade Federal de Minas Gerais Belo Horizonte, Brazil), pp 1–115.
77. Langner A, Siegert F (2009) Spatiotemporal fire occurrence in Borneo over a period of 10 years. *Glob Change Biol* 15:48–62.
78. Clement AC, Seager R, Cane MA (1999) Orbital controls on the El Niño/Southern Oscillation and the tropical climate. *Paleoceanography* 14:441–456.
79. Guilyardi E (2006) El Niño-mean state-seasonal cycle interactions in a multi-model ensemble. *Clim Dyn* 26:329–348.
80. Fairhurst T, McLeish M, Prasodjo R (2010) *Conditions Required by the Private Sector for Oil Palm Expansion on Degraded Land in Indonesia* (Tropical Crop Consultants Ltd, Wye, UK), pp 1–23.
81. Bonham-Carter G (1994) *Geographic Information Systems for Geoscientists: Modelling with GIS* (Pergamon, New York), pp 1–416.
82. Soares-Filho BS, Filho LC, Cerqueira GC, Araujo WL (2003) Simulating the spatial patterns of change through the use of the Dinamica model. *Anais XI* Simpósio Brasileiro de Sensoriamento Remoto, eds C BL and L RM (Instituto Nacional de Pesquisas Espaciais, Belo Horizonte, Brazil), pp 721–728.
83. Kaimowitz D, Angelsen A (1998) *Economic Models of Tropical Deforestation: A Review* (Center for International Forestry Research, Bogor, Indonesia), pp 1–139.
84. Geist HJ, Lambin EF (2002) Proximate causes and underlying driving forces of tropical deforestation. *Bioscience* 52:143–150.
85. Soares-Filho BS, et al. (2004) Simulating the response of land-cover changes to road paving and governance along a major Amazon highway: the Santarém-Cuiabá corridor. *Glob Change Biol* 10:745–764.
86. Almeida CM, Gleriani JM, Castejon EF, Soares BS (2008) Using neural networks and cellular automata for modelling intra-urban land-use dynamics. *Int J Geogr Inf Sci* 22: 943–963.
87. Hooijer A, Silvius M, Wösten H, Page S (2006) *PEAT-CO2: Assessment of $CO_2$ Emissions from Drained Peatlands in SE Asia*, Delft Hydraulics Report Q3943 (Delft Hydraulics, Delft, The Netherlands).
88. Dennis RA, Colfer CP (2006) Impacts of land use and fire on the loss and degradation of lowland forest in 1983-2000 in East Kutai District, East Kalimantan, Indonesia. *Singap J Trop Geogr* 27:30–48.
89. Page S, et al. (2009) Tropical peatland fires in Southeast Asia. *Tropical Fire Ecology: Climate Change, Land Use, and Ecosystem Dynamics*, ed Cochrane MA (Springer-Praxis Books, Chichester, UK), pp 263–287.

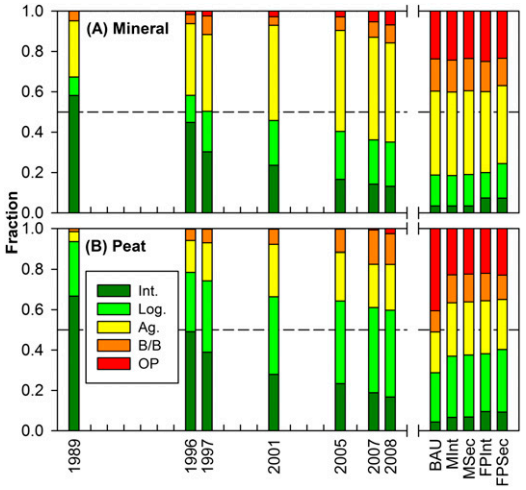


**Fig. S1.** (*A* and *B*) Land cover distribution (% area) across peat and mineral soils, 1989–2008 and projected through 2020 under five oil palm expansion scenarios. (*i*) Business-As-Usual (BAU) oil palm plantation expansion into allocated oil palm leases; a moratorium on oil palm expansion into (*ii*) intact (MInt) or (*iii*) intact, logged, and secondary (MSec) forests and peatlands in plantations established from 2012 to 2020; forest protection, identical to the moratorium scenarios with additional protection given to (*iv*) intact (FPInt) or (*v*) intact, logged, and secondary (FPSec) forests in oil palm leases and protected areas from 2011 to 2020. From 1989 to 2008, values were calculated from classified Landsat images. For scenarios, land cover distribution in 2020 was calculated as the mean of 20 model runs per scenario. Int., intact forest; Log., logged and secondary forest; Ag., agroforests and agricultural fallows; B/B, burned/cleared and bare; OP, oil palm plantations.

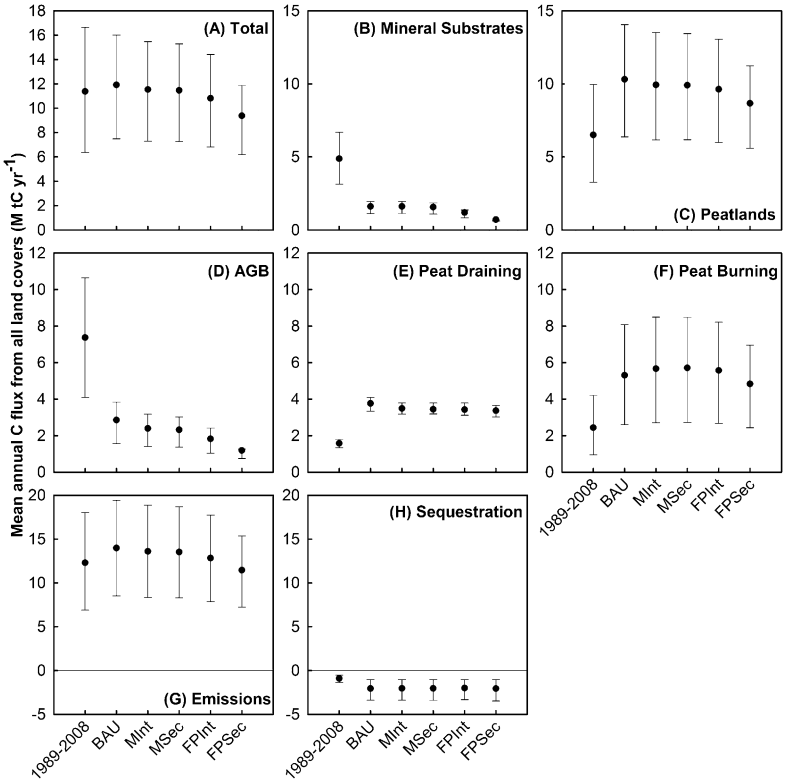


**Fig. S2.** (*A*–*H*) Mean annual carbon flux (MtC·y$^{-1}$) from all land covers for 1989–2008 and future scenarios 2008–2020 by substrate and pool. Positive values indicate net carbon emissions to the atmosphere, whereas negative values indicate net carbon sequestration. Error bars specify minimum and maximum mean annual estimated carbon flux derived by applying low carbon and high carbon input values. Low, mean, and high values represent the mean of 20 model runs per scenario with low, mean, or high carbon inputs.

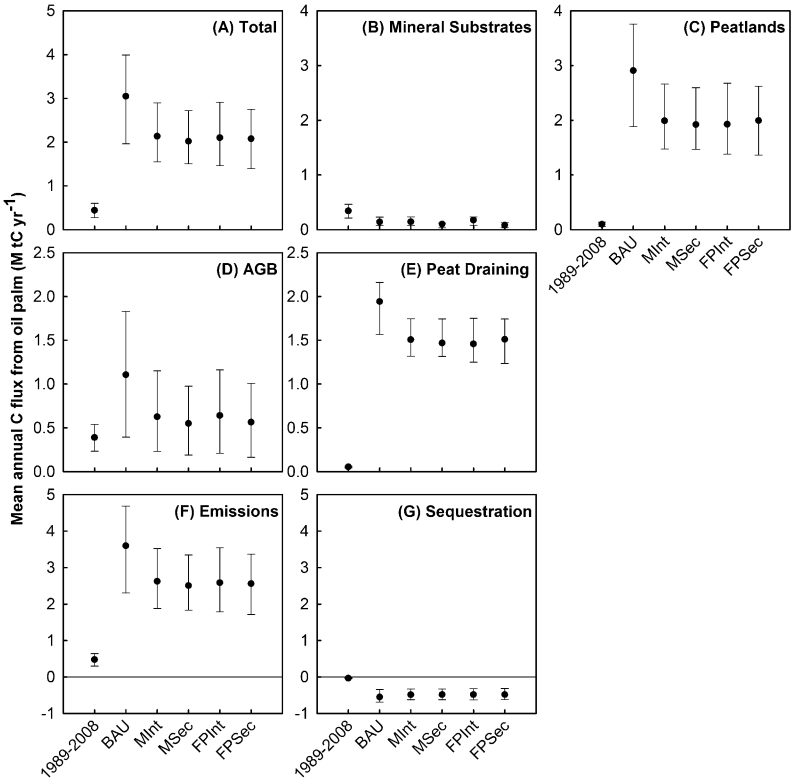


**Fig. S3.** (*A*–*G*) Mean annual carbon flux (MtC·y$^{-1}$) from oil palm for 1989–2008 and future scenarios by substrate and flux component. Positive values indicate net carbon emissions to the atmosphere, whereas negative values indicate net carbon sequestration. Error bars specify minimum and maximum mean annual estimated carbon flux derived by applying low carbon and high carbon input values. Low, mean, and high values represent the mean of 20 model runs per scenario with low, mean, or high carbon inputs.

**Table S1. Annual forest degradation (logging) and deforestation rates (%·y$^{-1}$) from 1989 to 2008**

| Transition | Substrate | 1989–1996 | 1996–1997 | 1997–2001 | 2001–2005 | 2005–2007 | 2007–2008 | 1989–2008 |
|---|---|---|---|---|---|---|---|---|
| Degradation, logging | Mineral | 1.9 | 16.6 | 3.7 | 4.5 | 3.3 | 8.2 | 4.1 |
| | Peat | 1.4 | 14.0 | 4.2 | 4.3 | 9.0 | 13.7 | 4.7 |
| | Overall | 1.6 | 15.1 | 4.0 | 4.4 | 6.7 | 11.6 | 4.5 |
| Deforestation | Mineral | 2.7 | 13.8 | 2.4 | 3.1 | 5.4 | 3.1 | 3.6 |
| | Peat | 2.5 | 5.4 | 2.8 | 0.8 | 2.5 | 2.3 | 2.3 |
| | Overall | 2.5 | 9.0 | 2.6 | 1.8 | 3.6 | 2.6 | 2.9 |
| | Oil palm | 0.1 | 0.4 | 0.1 | 0.0 | 0.5 | 0.7 | 0.2 |

"Degradation" is defined as any transition from intact forest to logged forest or secondary forest and any transition from secondary forest to logged forest. "Deforestation" is defined as any transition from intact, secondary, or logged forest to any other class (i.e., agroforest, burned/cleared, bare soil, or oil palm). The 1989–2008 rates were calculated as the mean of weighted rates for each period. Deforestation from conversion to oil palm plantations ("Oil palm") is a compilation of all transitions from intact, secondary, or logged forest classes to oil palm. Rates were derived by applying a compounding equation.

**Table S2. Aboveground live biomass (AGB) (tC·ha$^{-1}$) values used to model carbon flux from 1989 to 2008**

| | Mean | | | | Low | | | | High | | | |
|---|---|---|---|---|---|---|---|---|---|---|---|---|
| Land cover class | ≤300 m | >300 m | Peat | Δ | ≤300 m | >300 m | Peat | Δ | ≤300 m | >300 m | Peat | Δ |
| Intact forest | 401 | 292 | 180 | $AGB_{t1}$ | 255 | 191 | 71 | $AGB_{t1}$ | 547 | 393 | 288 | $AGB_{t1}$ |
| Logged, low | 281 | 204 | 126 | (0.07) $AGB_{t1}$ | 179 | 133 | 50 | (0.07) $AGB_{t1}$ | 383 | 275 | 202 | (0.07) $AGB_{t1}$ |
| Logged, high | 161 | 117 | 72 | (0.04) $AGB_{t1}$ | 102 | 76 | 28 | (0.04) $AGB_{t1}$ | 219 | 157 | 115 | (0.04) $AGB_{t1}$ |
| Secondary forest | 161 | 117 | 72 | (1.02) $AGB_{t1}$ | 102 | 76 | 28 | (1.01) $AGB_{t1}$ | 219 | 157 | 115 | (1.03) $AGB_{t1}$ |
| Agroforest, young | 0 | 0 | 0 | −10.12 + (3.18) $A$ | 0 | 0 | 0 | −10.12 + (2.42) $A$ | 0 | 0 | 0 | −10.12 + (3.95) $A$ |
| Agroforest, mature | 22 | 22 | 0 | −10.12 + (3.18) $A$ | 14 | 14 | 0 | −10.12 + (2.42) $A$ | 29 | 29 | 0 | −10.12 + (3.95) $A$ |
| Burned and cleared | 0 | 0 | 0 | 0 | 0 | 0 | 0 | 0 | 0 | 0 | 0 | 0 |
| Bare soil and built | 0 | 0 | 0 | 0 | 0 | 0 | 0 | 0 | 0 | 0 | 0 | 0 |
| Oil palm | 0 | 0 | 0 | (5.97) $A^{0.62}$ | 0 | 0 | 0 | 13.57 + (1.83) $A$ + (−0.003) $A^2$ | 0 | 0 | 0 | −2.7 + (2.35) $A$ + (−0.04) $A^2$ |

Mean, low, and high input values offer bounds on carbon flux estimates from land cover change. To initialize the model for intact forests on mineral soils, we used estimates collected in the Ketapang region on alluvial (≤300 m) and granitic (>300 m) soils (1). For intact forests on peat substrates, we used estimates from Sumatra and Kalimantan (39). Initial logged forest biomass was calculated by debiting intact forest AGB by 30% for low-intensity logged forest and 60% for high-intensity logged forests. Secondary forests were initially assigned the same biomass as high-intensity logged forests. Young agroforests (<10 y) were conservatively assigned 0 AGB, whereas initial AGB for mature agroforests (≥10 y) was derived from AGB-age relationships at age 10, developed for rice fallows in Ketapang (14). Change (Δ) in AGB at time t2 was calculated by modifying AGB at t1 (intact forests, secondary forests, logged forests) or based on relationships between vegetation age ($A$) and AGB (agroforests, oil palm). Burned/cleared and bare soil areas were assigned an AGB of zero. Oil palm and agroforest land cover classes were assigned 0 tC·ha$^{-1}$ AGB for ages <4 y.

**Table S3. Net carbon emissions generated from peatland burning**

| Variable | Mean | Low | High |
|---|---|---|---|
| Peat depth, m | 0.33 | 0.15 | 0.51 |
| Peat bulk density, $g \cdot cm^{-3}$ | 0.11 | 0.09 | 0.13 |
| Peat C content, % | 56 | 54 | 58 |
| Volumetric C density, $tC \cdot m^{-3}$ | 0.06 | 0.05 | 0.08 |
| Peat C density, $tC \cdot ha^{-1} \cdot m^{-1}$ | 615 | 480 | 757 |
| C loss from fire, $tC \cdot ha^{-1} \cdot burn^{-1}$ | 203 | 72 | 386 |

All values are derived from data collected in Sumatra and Kalimantan by Shimada et al. (68) except burn depth, measured by Ballhorn et al. (71). Mean, low, and high input values offer bounds on carbon flux estimates from land use change.

**Table S4. Net carbon emissions (tC $ha^{-1}$ $yr^{-1}$) from drained peatlands**

| Land Cover | Location | C Emissions | Source |
|---|---|---|---|
| Agriculture | Jambi | 21.00 | (38) |
| Agriculture (Cassava) | Jambi | 17.45 | (64) |
| Agriculture (Wet Rice) | Central Kalimantan | 15.40 | (73) |
| Agriculture (Wet Rice) | South Kalimantan | 13.98 | (74) |
| Agriculture (Sago) | Sarawak | 11.10 | (75) |
| Burned/Cleared | Jambi | 16.91 | (38) |
| Oil Palm | Sarawak | 15.40 | (75) |
| | *Mean ± SD* | *15.89 ± 3.07* | |

Peat emissions depend on drainage depth, which varies within and between land cover classes. Thus, for all non-forested peatlands (i.e., agroforests and agricultural fallows, burned/cleared, bare soil, and oil palm) we calculated the mean emission rate from closed-chamber $CO_2$ flux studies in Borneo and Sumatra.